Chapter 2: Sensor Characteristics and Physical Effects

2.1 Introduction

The potential of nanotechnology enabled sensors was highlighted in the previous chapter. In this chapter, the fundamental characteristics and terminologies associated with transducers and sensors are introduced. Furthermore, some of the major effects that are utilized in sensing for the conversion of energy from a measurand (the physical parameter being quantified by a measurement) to a measurable signal are described. These effects illustrate the relationship between different physical and chemical phenomena that can be measured using sensors. This will be a prelude to Chap. 3, which focuses on major transduction platforms.

The essence of Chap. 2 is on physical transduction phenomena. The majority of chemical phenomena which are related to nanotechnology enabled sensing can be found in Chaps. 6 and 7.

2.2 Sensor Characteristics and Terminology

A *sensor* is a device that produces a measurable signal in response to a stimulus. A *transducer* is a device that converts one form on energy into another. Generally, a sensing or sensitive layer/medium directly responds to the external stimulus, while the transducer converts the response into an external measurable quantity. As distinct from *detectors,* sensors are employed to monitor and quantify changes in the measurand, whereas detectors simply indicate the presence of the measurand.[1,2]

The characteristics of a sensor may be classified as being either *static*, or *dynamic*. These parameters are essential in high fidelity mapping of output versus input. Static characteristics are those that can be measured after all transient effects have stablized to their final or steady state. They address questions such as; by how much did the sensor's output change in response

to the input? what is the smallest change in the input that will give an output reading? and how long did it take for the output value to change to the present value? Dynamic characteristics describe the sensor's transient properties. These typically address questions such as; at what rate is the output changing in response to the input? and what impact would a slight change in the input conditions have on the transient response?

2.2.1 Static Characteristics

Accuracy:

This defines how correctly the sensor output represents the true value. In order to assess the accuracy of a sensor, either the measurement should be benchmarked against a standard measurand or the output should be compared with a measurement system with a known accuracy. For instance, an oxygen gas sensor, which operates at a room with 21% oxygen concentration, the gas measurement system is more accurate if it shows 21.1% rather than 20.1% or 22%.

Error:

It is the difference between the true value of the quantity being measured and the actual value obtained from the sensor. For instance, in the gas sensing example, if we are measuring the oxygen content in the room having exactly 21% oxygen, and our sensor gives us a value of 21.05%, then the error would be 0.05%.

Precision:

Precision is the estimate which signifies the number of decimal places to which a measurand can be reliably measured. It relates to how carefully the final measurement can be read, not how accurate the measurement is.

Resolution:

Resolution signifies the smallest incremental change in the measurand that will result in a detectable increment in the output signal. Resolution is strongly limited by any noise in the signal.

Sensitivity:

Sensitivity is the ratio of incremental change in the output of the sensor to its incremental change of the measurand in input. For example, if we

have a gas sensor whose output voltage increases by 1 V when the oxygen concentration increases by 1000 ppm, then the sensitivity would be 1/1000 V/ppm, or more simply 1 mV/ppm.

Selectivity:

A sensor's ability to measure a single component in the presence of others is known as its selectivity. For example, an oxygen sensor that does not show a response to other gases such as CO, CO_2 and NO_2, may be considered as selective.

Noise:

Noise refers to random fluctuations in the output signal when the measurand is not changing. Its cause may be either internal or external to the sensor. Mechanical vibrations, electromagnetic signals such as radio waves and electromagnetic noise from power supplies, and ambient temperatures, are all examples of external noise. Internal noises are quite different and may include:

1. *Electronic Noise*, which results from random variations in current or voltage. These variations originate from thermal energy, which causes charge carriers to move about in random motions. It is unavoidable and present in all electronic circuits.
2. *Shot Noise*, which manifests as the random fluctuations in a measured signal, caused by the signal carriers' random arrival time. These signal carriers can be electrons, holes, photons, etc.
3. *Generation-Recombination Noise*, or *g-r noise*, that arises from the generation and recombination of electrons and holes in semiconductors.
4. *Pink Noise*, also known as *1/f noise*, is associated with a frequency spectrum of a signal, and has equal power per octave. The noise components of the frequency spectrum are inversely proportional to the frequency. Pink noise is associated with self-organizing, bottom-up systems that occur in many physical (e.g. meteorological: thunderstorms, earthquakes), biological (statistical distributions of DNA sequences, heart beat rhythms) and economical systems (stock markets).

Drift:

It is the gradual change in the sensor's response while the measurand concentration remains constant. Drift is the undesired and unexpected change that is unrelated to the input. It may be attributed to aging,

temperature instability, contamination, material degradation, etc. For instance, in a gas sensor, gradual change of temperature may change the baseline stability, or gradual diffusion of the electrode's metal into substrate may change the conductivity of a semiconductor gas sensor which deteriorating its baseline value.

Minimum Detectable Signal (*MDS*)*:*

This is the minimum detectable signal that can be extracted in a sensing system, when noise is taken into account. If the noise is large relative to the input, it is difficult to extract a clear signal from the noise.

Detection Limit:

It is the smallest magnitude of the measurand that can be measured by a sensor.

Repeatability:

Repeatability is the sensor's ability to produce the same response for successive measurements of the same input, when all operating and environmental conditions remain constant.

Reproducibility:

The sensor's ability to reproduce responses after some measurement condition has been changed. For example, after shutting down a sensing system and subsequently restarting it, a reproducible sensor will show the same response to the same measurand concentration as it did prior to being shut down.

Hysteresis:

It is the difference between output readings for the same measurand, when approached while increasing from the minimum value and the other while decreasing from the peak value.

Stability:

The sensor's ability to produce the same output value when measuring a fixed input over a period of time.

Response Time:

The time taken by a sensor to arrive at a stable value is the response time. It is generally expressed as the time at which the output reaches a

certain percentage (for instance 95%) of its final value, in response to a stepped change of the input. The *recovery time* is defined in a similar way but conversely.

Dynamic Range or Span:

The range of input signals that will result in a meaningful output for the sensor is the dynamic range or span. All sensors are designed to perform over a specified range. Signals outside of this range may be unintelligible, cause unacceptably large inaccuracies, and may even result in irreversible damage to the sensor.

2.2.2 Dynamic Characteristics

It is advantageous to use *linear* and *time invariant* mathematical representations for sensing systems. Such representations have been widely studied, they are easy to extract information from and give an overall vision about the sensing systems to the users. The relationship between the input and output of any linear time invariant measuring system can be written as:

$$a_n \frac{d^n y(t)}{dt^n} + a_{n-1} \frac{d^{n-1} y(t)}{dt^{n-1}} + \ldots + a_1 \frac{dy(t)}{dt} + a_0 y(t) = b_m \frac{d^{m-1} x(t)}{dt^m} + b_{m-1} \frac{d^{m-1} x(t)}{dt^{m-1}} + \ldots + b_1 \frac{dx(t)}{dt} + b_0 x(t) \quad , \tag{2.1}$$

where $x(t)$ is the measured quantity (input signal) and $y(t)$ is the output reading and $a_0, \ldots, a_n, b_o, \ldots, b_m$ are constants.

$x(t)$ can have different forms and values. As a simple and commonly encountered example in sensing systems, $x(t)$ may be considered to be a *step change* (*step function*) similar to that depicted in **Fig. 2.1**. However, on many occasions this is an over simplification, as there is generally a rise and fall time for the step input to occur.

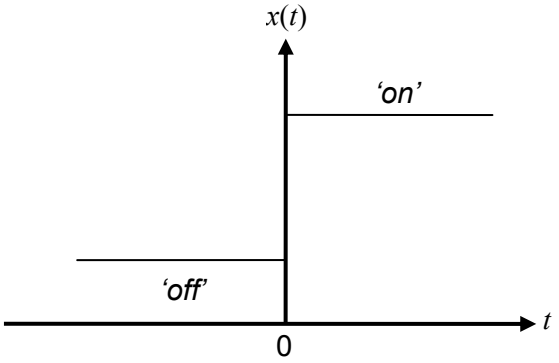

Fig. 2.1 A step change.

When the input signal is a step change, Eq. (2.1) reduces to:

$$a_n \frac{d^n y(t)}{dt^n} + a_{n-1} \frac{d^{n-1} y(t)}{dt^{n-1}} + \ldots + a_1 \frac{dy(t)}{dt} a_{n-1} + a_0 y(t) = b_0 x(t), \tag{2.2}$$

as all derivatives of $x(t)$ with respect to t are zero. The input does not change with time except at $t = 0$. Further simplifications can be made. For instance, if output shows an instantaneous response to the input signal then all $a_1, \ldots, a_n$ coefficients except a_0 are zero, as a result:

$$a_0 y(t) = b_0 x(t) \text{ or simply: } y(t) = Kx(t). \tag{2.3}$$

where $K = b_0/a_0$ is defined as the static sensitivity. Such a response represents a perfect zero order system. If the system is not perfect and the output does show a gradual approach to its final value, then it is called a first order system. A simple example of a first order system is the charging of a capacitor with a voltage supply, whose rate of charging is exponential in nature. Such a first order system is described by the following:

$$a_1 \frac{dy(t)}{dt} + a_0 y(t) = b_0 x(t), \tag{2.4}$$

or after rearranging:

$$\frac{a_1}{a_0} \frac{dy(t)}{dt} + y(t) = \frac{b_0}{a_0} x(t). \tag{2.5}$$

By defining $\tau = a_1/a_0$ as the time constant, the equation will take the form of a *first order ordinary differential equation* (*ODE*):

$$\tau \frac{dy(t)}{dt} + y(t) = Kx(t)\,. \tag{2.6}$$

This ODE can be solved by obtaining the homogenous and particular solutions. Solving this equation reveals that the output $y(t)$ in response to $x(t)$ changes exponentially. Furthermore, τ is the time taken for the output value to reach 63% of its final value, i.e. $(1\text{-}1/e^{-1}) = 0.6321$, as seen in a typical output of a first order system in **Fig. 2.2**.

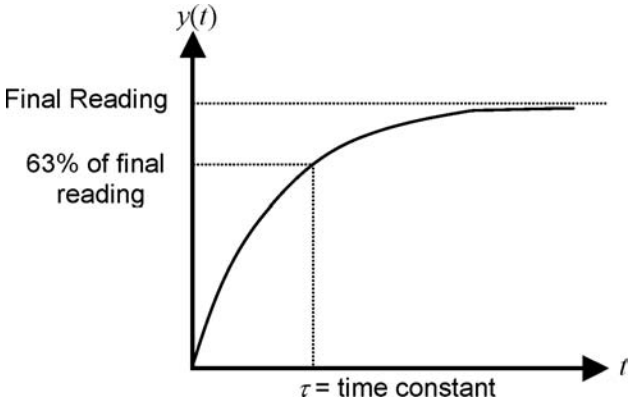

Fig. 2.2 Graphical depiction of a first order system's response with a time constant of τ.

On the other hand, the response of a *second order system* to a step change can be defined as:

$$a_2 \frac{d^2y(t)}{dt^2} + a_1 \frac{dy(t)}{dt} + a_0 y(t) = b_0 x(t)\,. \tag{2.7}$$

By defining the undamped natural frequency $\omega = a_0/a_2$, and the damping ratio $\varepsilon = a_1/(2a_0a_2)$, Eq. (2.7) reduces to:

$$\frac{1}{\omega^2}\frac{d^2y(t)}{dt^2} + \frac{2\varepsilon}{\omega}\frac{dy(t)}{dt} + y(t) = Kx(t)\,. \tag{2.8}$$

This is a standard second order system. The damping ratio plays a pivotal role in the shape of the response as seen in **Fig. 2.3**. If $\varepsilon = 0$ there is no damping and the output shows a constant oscillation, with the solution being a sinusoid. If ε is relatively small then the damping is light, and the oscillation gradually diminishes. When $\varepsilon = 0.707$ the system is *critically*

damped. A critically damped system converges to zero faster than any other without oscillating. When ε is large the response is heavily damped or *over damped*. Many sensing systems follow the second order equations. For such systems responses that are not near the critically damped condition ($0.6 < \varepsilon < 0.8$) are highly undesirable as they are either slow or oscillatory.[3]

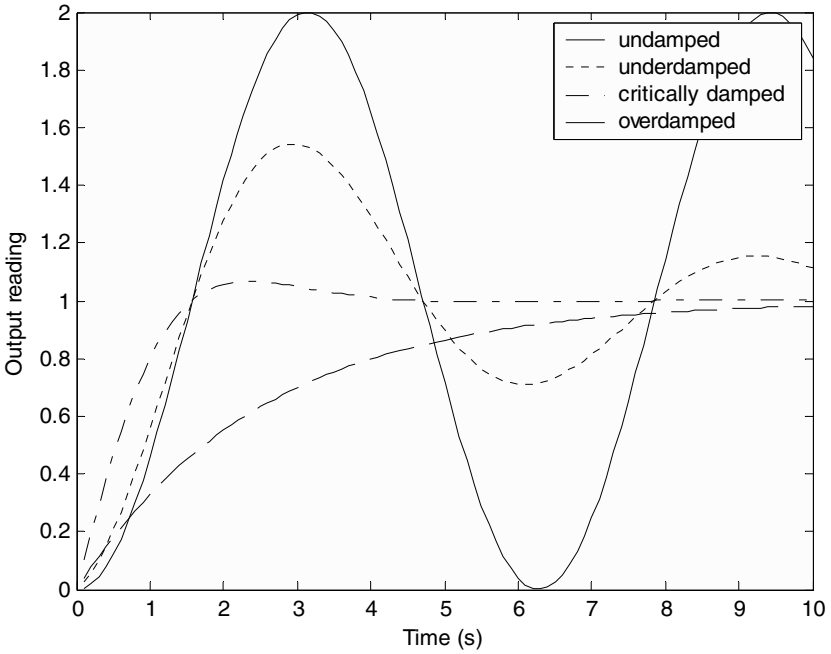

Fig. 2.3 Responses of second order systems to a step input.

2.3 Physical Effects Employed for Signal Transduction

Physical effects employed for signal transduction generally involve the coupling of a material's *thermal*, *mechanical* and *electromagnetic* (including *optical*) properties. **Table 2.1** shows examples of effects that are obtained when thermal, mechanical and electromagnetic properties are coupled with each other, or with themselves.

Within the above mentioned physical effects, *chemical interactions* may also be involved. In chemical reactions thermal, mechanical and electromagnetic energies are released or absorbed.

In the subsequent sections, some of the most widely utilized physical effects in sensor technology, along with several examples relevant to nanotechnology enabled sensing, are provided.

Table 2.1 Some well known physical effects.

Physical effect	Thermal	Mechanical	Electromagnetic (including optical)
Thermal	e.g. heat transfer	e.g. thermal expansion	e.g. thermoresistance
Mechanical	e.g. friction	e.g. acoustic effects	e.g. magnetostriction
Electromagnetic (including optical)	e.g. Peltier effect	e.g. piezoelectricity	e.g. Hall and Faraday effects

2.3.1 Photoelectric Effect

When a material is irradiated by photons, electrons may be emitted from the material. The ejected electrons are called *photoelectrons*, and their kinetic energy, E_K, is equal to the incident photon's energy, hv, minus a threshold energy, known as the material's *work function* ϕ, which needs to be exceeded for the material to release electrons. The effect is illustrated in **Fig. 2.4** and is governed by Eq. (2.9):

$$E_K = hv - \phi, \tag{2.9}$$

where h is Planck's constant ($h = 6.625\times10^{-34}$ Js) and v is the photon's frequency.

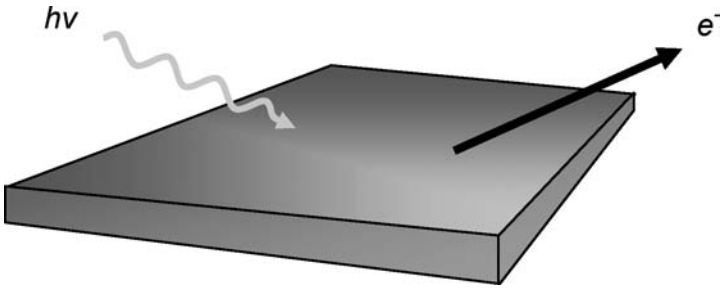

Fig. 2.4 Photoelectric effect.

The photoelectric effect is ideal for use in light sensitive devices. Because the work function depends on the material, sensors may be designed that are tuned to specific wavelengths. Electrodes with nanostructured surfaces have emerged as excellent candidates for use in photoelectric devices and sensors. The work function can be tuned by changing of the material's dimensions. The large surface to volume ratio nanostructures may enhance the photoelectric device's light-to-energy conversion efficiency (Chap. 6). In addition, the release of produced charges is faster in nanomaterials, which translates into a faster device response.[4] Related to this effect are the *photoconductive* and the *photovoltaic* effects.

Photoconductive Effect

Photoconductivity occurs when a beam of photons impinges on a semiconducting material, causing its conductivity to change. The conductivity results from the excitation of free charge carriers caused by the incident photons, which occurs if the light striking the semiconductor has sufficient energy. This effect is widely utilized in electromagnetic radiation sensors, and such devices are termed *photoconductors*, *light-dependent resistors* (*LDR*) or *photoresistors*.

Cadmium sulfide (CdS) and cadmium selenide (CdSe) are the two most common materials for the fabrication of photoconductive devices and sensors (see **Fig. 2.5**).[5] Devices based on CdS can have a wide range of resistance values, from approximately a few ohms when the light has high intensity, to several mega ohms in darkness. They are capable of responding to a broad range of photon frequencies, including infrared, visible, and ultraviolet.

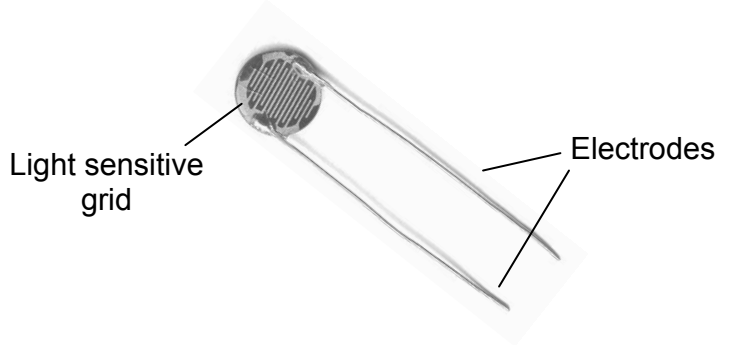

Fig. 2.5 Photo of a commercial LDR based on CdS.

Nanomaterials are currently being employed in photoconductive devices to improve their sensitivity, efficiency and response times. Semiconduct-

ing nanomaterials exhibit a charge depletion layer, which extends a few nanometers. This extension of the depletion region changes when exposed to irradiation. Depending on their dimensions and the amount of doping, photosensitive devices may become completely depleted of charge when irradiated. For instance, the photocurrent resulting from the interaction of UV light and semiconducting GaN-nanowires is seen in Fig. 2.6, where a distinct dependence on the nanowires diameter is observed.[6]

The response of photoconductive devices may also be tuned by varying the composition and dimensions of the utilized nanomaterials. This is seen in devices based on CdS and CdSe nanoparticles and nanostructured thin films for applications such as *Tera Hertz* (*THz*) signal monitoring.[7,8] The size-dependent transient photoconductivity of CdSe nanoparticles using time-resolved THz spectroscopy (TRTS) is shown in **Fig. 2.7**, which reveals the response time is reduced to less than 5 ps when the nanoparticle sizes are reduced to approximately 3.5 nm.

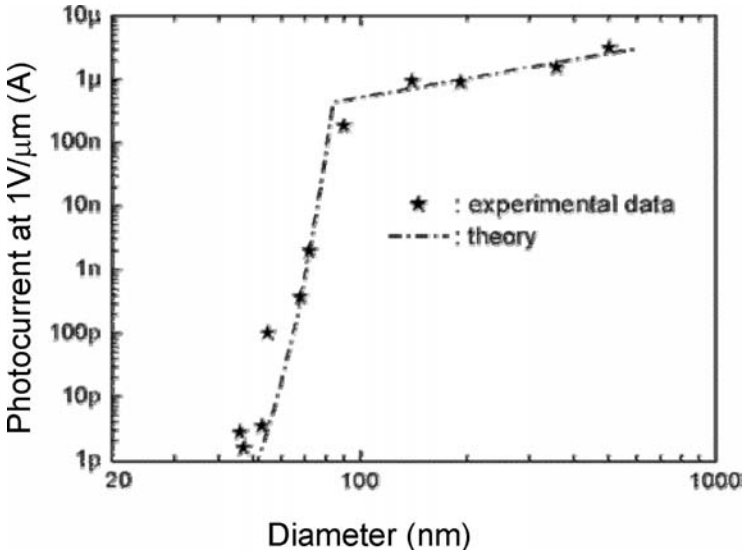

Fig. 2.6 Photocurrent with UV illumination of approximately 15 W/cm^2 versus diameter. The kink in the fitting curve at 85 nm indicates the critical diameter where the surface depletion layer just completely depletes the nanowire. For smaller diameters the photocurrent shows an exponential decrease, for larger diameters the photocurrent is proportional to the diameter. Reprinted with permission from the American Chemical Society publications.[6]

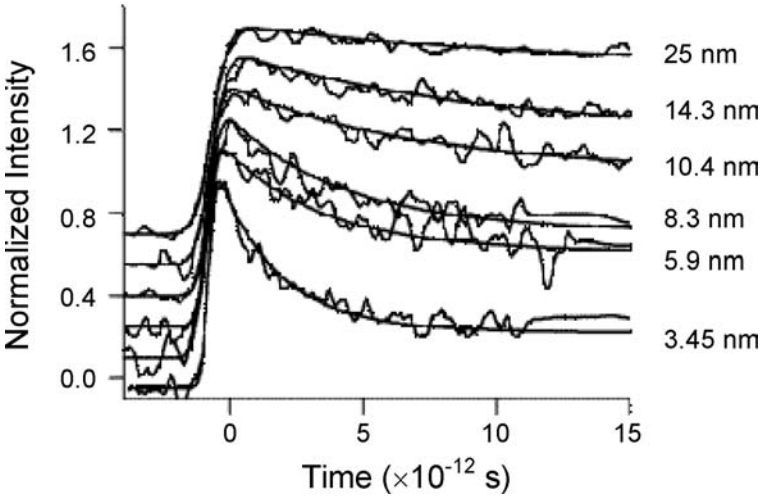

Fig. 2.7 TRTS scans for the eight sizes of CdSe nanoparticles, normalized and offset from the smallest to the largest size nanoparticles. Reprinted with permission from the American Chemical Society publications.[7]

Photovoltaic Effect

In the *photovoltaic effect*, a voltage is induced by the absorbed photons at a junction of two dissimilar materials (*heterojunction*). The absorbed photons produce free charge carriers. The induced voltage in the heterojunction causes the charge carriers to move, resulting in current flow in an external circuit. Materials used for fabricating such heterojunctions are typically semiconductors.

A typical photovoltaic device is seen in **Fig. 2.8**. They generally consist of a large area semiconductor *p-n junction* or diode. A photon impinging on the junction is absorbed if its energy is greater than or equal to the semiconductor's bandgap energy. This can cause a valance band electron to be excited into the conduction band, leaving behind a hole, and thus creating a mobile electron-hole pair. If the electron-hole pair is located within the depletion region of the *p-n* junction, then the existing electric field will either sweep the electron to the *n*-type side, or the hole to the *p*-type side. As a result, a current is created that is defined by:

$$I = I_S[e^{qV/kT} - 1], \tag{2.10}$$

where q is the electron charge (1.602×10^{-19} C), k is Boltzmann's constant (1.38×10^{-23} J/K), and T is the temperature of the *p-n* junction in Kelvin.

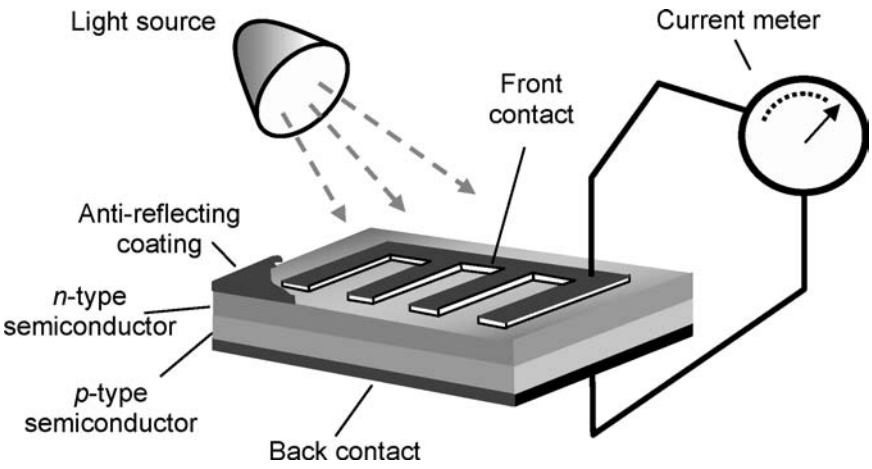

Fig. 2.8 Diagram of a photovoltaic device.

Photovoltaic cells and sensors are commonly made from materials that absorb photons in the visible and UV ranges, such as GaAs (gallium arsenide - band gap 1.43 eV) and compounds thereof. For other wavelength ranges, materials such as: silicon (wavelengths between 190-1100 nm), germanium (800-1700 nm), indium galium arsenide (800-2600 nm), and lead sulfide (1000-3500 nm) are generally used.

Photovoltaic devices can be employed in a wide range of sensing applications. These include use in analytical apparatus such as spectrophotometers, radiation monitors, automatic light adjustment systems in buildings, as light sensors in optical communication systems, etc. Photovoltaic devices are also the basis of photovoltaic cells for the generation of power from solar energy.

Important factors to be considered when designing photovoltaic devices and sensors are efficiency and cost. Such devices are generally inefficient, with efficiency varying from 5% for amorphous silicon-based devices to 35% or higher with *multiple-junction cells* used in research labs.[9] To overcome this, much research is being devoted to multi-junction cells based on thin films with thicknesses measuring a few nanometers. For sensing applications, GaAs is the material of choice as it is relatively insensitive to heat and devices have been made with efficiencies as high as 35.2%.[9]

Research is currently being focused on increasing their sensitivity and performance through the incorporation of nanodimensional structures and materials. The unique advantage of using nanomaterials in photovoltaic

devices and sensors include: small effective cross-sections which leads to small capacitance and large mobility of carriers.[10] The combination of very short transit time of the photo-generated carriers with a small capacitance can be implemented for ultra high-speed sensing.[11] A large breakdown voltage and wider depletion region can also be obtained for such sensors because of the spread electric field streamlines.[12]

The range of wavelengths absorbed depends on material's electronic properties. These are not only determined by the material's composition, but also on in its dimensions. For example, devices with tunable absorption wavelengths comprised of carbon nanotubes[13] or semiconducting nanocrystals embedded into polymer matrices[14] have already been developed. Some of the most promising nanomaterials currently being researched are cadmium telluride (CdTe)[15,16] and copper indium gallium selenide (CIGS).[17] These photovoltaic devices are based on a thin film hetero-junctions structures and their efficiency is approximately 19.5%.

Nanostructured organic semiconductors and conductive polymers are also being developed for use in photoconducive devices.[18-20] However, devices and sensors made from them generally suffer from degradation upon exposure to UV light, resulting in short lifetimes, a serious concern for commercial applications. Inorganic semiconductor-based nanomaterials have superior performance due to their intrinsically higher carrier mobilities. Charges may be transported to the electrodes more quickly, reducing current losses through recombination and improving their dynamic performance.[21]

Combining polymeric materials with inorganic semiconductors nanoparticles has been shown to overcome charge transport limitations.[21] Charge transfer is favored between high electron affinity inorganic semiconductors and the relatively low ionization potential inherent in organic molecules. Charge transfer rates can be remarkably increased in the case of organics that are chemically bound to nanocrystalline and bulk inorganic semiconductors, which have a high density of electronic states. The combination of such materials is promising for the development of future generation photovoltaic cells and sensors.

Other developments in photovoltaic cells and sensor include the *dye-sensitized* based devices (also called *photoelectrochemical cells* or *Graetzel cells*), which mimic the photosynthesis process.[22,23] Their structure depends on a layer of nano porous material such as titanium dioxide and dye molecules that absorb light. The photo-generated electrons flow into the TiO_2 layer while the holes flow into an electrolyte on the other side of the dye. Unfortunately, the longevity of such devices is limited, because organic dyes currently utilized suffer form photo-degradation.

2.3.2 Photodielectric Effect

Materials whose dielectric properties change when illuminated by radiant energy are called photodielectric. Photodielectric measurements have been widely employed in photochemistry as in the study of kinetics in photographic materials and semiconductors.[24] It serves as a non-contact approach to measure a material's photoconductivity in an alternating electric field, and can be applied to complex semiconductors for which growth of monocrystals is difficult to monitor.[25] More on photodielectric effect and the integration of nanomaterials will be presented in Chap. 6.

2.3.3 Photoluminescence Effect

In photoluminescence effect, light is emitted from atoms or molecules after they have absorbed photons.[26] The absorbed photons give their energy to the molecule, causing it to change to a higher energy state. Then after some time, the molecule radiates the excess energy back out in the form of a photon, and it consequently returns to a lower energy state. The energy of the emitted light relates to the difference in energy levels of the excited state and the equilibrium state. *Fluorescence* and *phosphorescence* are examples of photoluminescence.

Photoluminescence can be explained with quantum mechanics. It depends on the *electronic structure* of atoms and molecules. Molecules have electronic states, and within each there are different *vibrational levels*, and within each vibrational level there exist *rotational levels*. After accepting energy in the form of a photon, an electron is raised to a permitted electronic state higher up. For most molecules, the *electronic states* can be divided into *singlet* (S) and *triplet* (T) states, depending on the electron spin. After a molecule is excited to a higher electronic energy state, it loses its energy quite rapidly via a number of pathways (**Fig. 3.31**).

In fluorescence, vibrational relaxation brings the molecule to its lowest vibrational energy level, $V' = 1$, in the first excited singlet state, S_1. Consequently, the electron relaxes from the lowest vibrational energy level in S_1 to any vibrational level of S_0.[27,28] For phosphorescence, the electron in S_1 undergoes *intersystem crossing* to T_1 and then relaxes to S_0.[29]

Due to the multiple rearrangements during the process, the phosphorescence has much longer lifetime than the fluorescence. For fluorescence, the period between absorption and emission is typically between 10^{-8} and 10^{-4} s. However for phosphorescence, this time is generally longer (10^{-4} to 10^{2} s).[30]

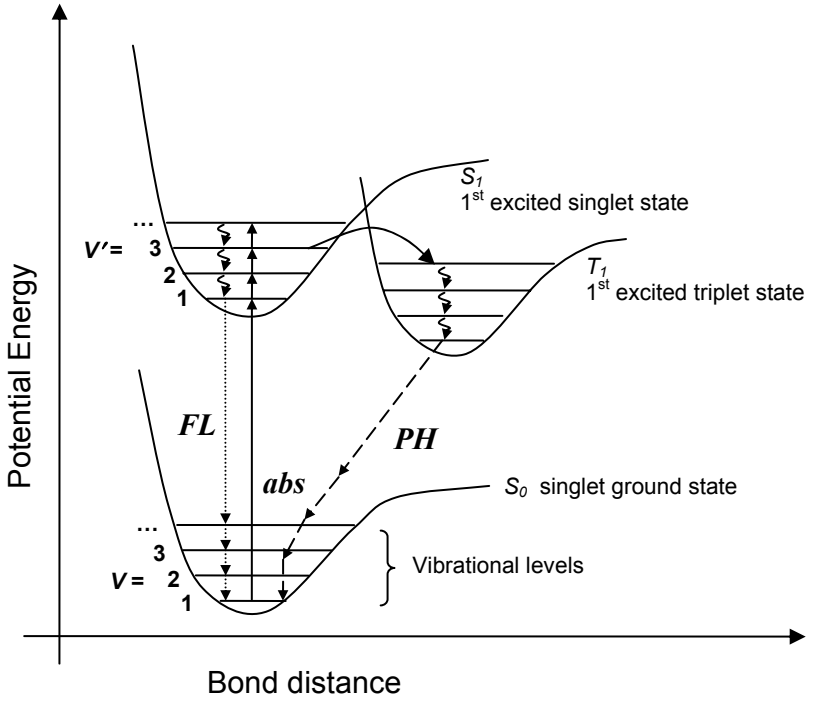

Fig. 2.9 Fluorescence and phosphorescence processes.

Organic molecules that exhibit fluorescence find many applications in nanotechnology enabled sensing. For example, fluorescence probes are used in biotechnology as a tool for monitoring biological events in individual cells. Other molecules are used as *ion probes*, in which after interacting with ions such that are important in neurological processes (e.g. Ca^{2+}, Na^{+}, etc.) their photoluminescence properties such as absorption wavelength, emission wavelength or emission intensity may change. In fact, these changes have been utilized to quantify events that take place in different parts of individual neurons. An example of this can be seen **Fig. 2.10**. Here fluorescence has been employed to image tumor-associated lysosomal protease using the *near-infrared fluorescence* (*NIRF*) probes[31]. Such probes generally have sub-micron dimensions and commercially available in different types and emission spectra.

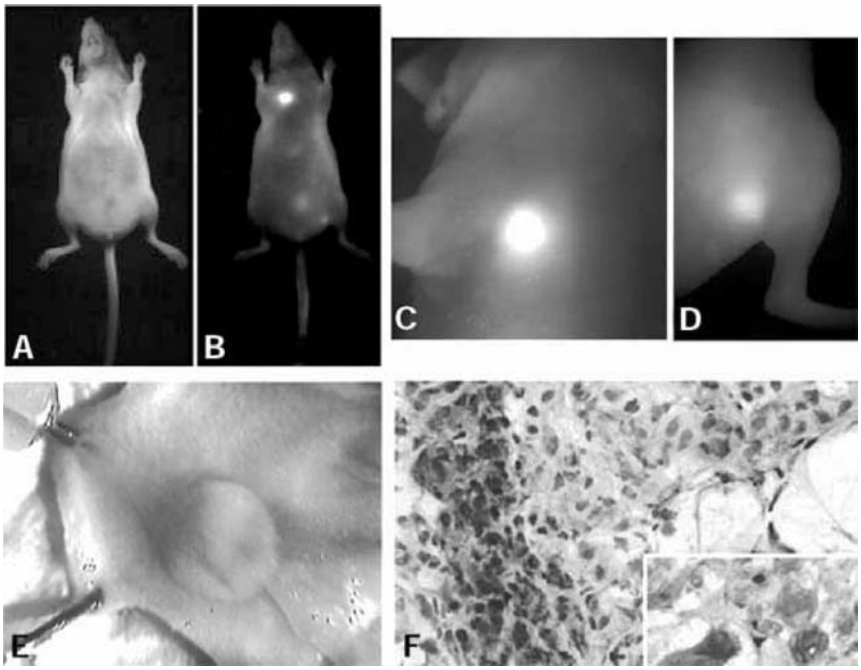

Fig. 2.10 LX-1 tumor implanted into the mammary fat pad of a nude mouse: (A) Light image. (B) Raw NIRF image. Note the bright tumor in the chest. (C) High resolution NIRF image of the chest wall tumor (2 mm). (D) High resolution NIRF image of the additional thigh tumor (<0.3 mm). (E) Dissected tumor in the mammary pad. (F) Hematoxylin-eosin section of the NIRF positive tumor showing malignant and actively proliferating cells (magnification 200; insert 400). Reprinted with permission from the Nature publications.[31]

Many inorganic molecules also exhibit photoluminescence properties that are extremely useful for probing and in nanotechnology enabled sensing. Some of the most popular of such particles are small zero dimensional semiconducting nanocrystals, also called *quantum dots* (*Q-dots*). They exhibit quantum confinement effects when their dimensions are smaller than *Bohr's radius*, which occurs at around 10 nm or less.

One of advantages of utilizing Q-dots in sensing applications is their size and material dependent photoluminescence properties. For example, ZnS nanocrystals have large band gaps and hence lower emission wavelengths whilst CdS nanocrystals have narrower band gaps and higher emission wavelengths. Furthermore, the emission wavelength can be tuned by simply changing the size of the nanocrystals, whilst using the same wavelength for their excitation.[32] Q-dots also have very narrow emission bands,

considerably narrower than those of organic photoluminescent molecules, and their emission lifetime can be much longer ($> 10^{-4}$ s). However, they are much larger than conventional fluorescent organic molecules, whose dimensions are generally in the angstrom, not nanometer, range.

Q-dots can be employed for bioimaging,[33,34] and biomolecules such as antibodies (**Fig. 2.11**) can also be attached to them for sensing applications.[35] In such cases the biomolecules carry the Q-dots to specific sites either on the cell surface or inside it, after which they can be probed. In biological applications, they have the added benefit of not being subject to microbial attack. Additionally, by attaching different sized Q-dots of the same material to organic biomolecules, multiple emission wavelengths, colors, can be employed to probe different biological events simultaneously whilst using the a single excitation wavelength. This quality is difficult to achieve with organic photoluminescent molecules, as each of them generally requires a different laser wavelength to activate its fluorescence.

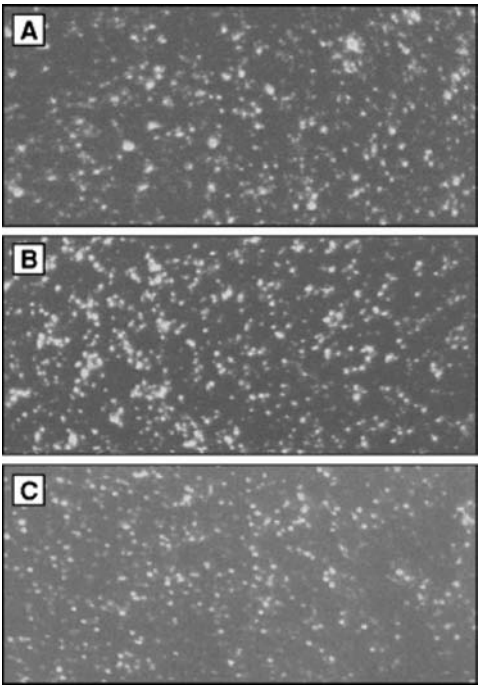

Fig. 2.11 Luminescence images obtained from (A) original Q-dotss, (B) mercapto-solubilized Q-dots, and (C) Q-dotes IgG conjugates (Q-dots conjugates and their interactions with biomaterials will be described in Chap. 7). Reprinted with permission from the Science Magazine publications.[35]

2.3.4 Electroluminescence Effect

Electroluminescence occurs when a material emits light as a result of an electrical current flowing through it, or when subjected to an electrical potential. It is used in the conversion of electrical energy into radiant energy. There are two methods of producing electroluminescence. Firstly, it can occur when a current passes through boundary of highly doped junctions (such as *p-n* junctions of semiconductor materials). Electrons can recombine with holes, causing them to fall into a lower energy level and release energy in the form of photons. Such a device is called *light-emitting diode* (*LED*) and its layout is shown in **Fig. 2.12**.

Electroluminescent devices can be implemented in spectroscopy and integrated sensors. Many new disposable sensors with the light intensity as the measure of a target analyte concentration or a physical change make use of them. This effect is an integrated part of many electrochemical sensing system (electrochemical sensing templates will be presented in Chap. 3). When an electron is generated in an electrochemical interaction it can transformed into a photon via the usage of an electroluminescent device. Consequently, this irradiation can be detected with a photodiode or photo transistor. The use of optical reading reduces the electronic noise and also it is compatible with many standard optical sensing systems.

The wavelength of the emitted light is determined by the bandgap energy of the materials forming the junction. A flow of a current does not guarantee electroluminescence. For example, in diodes based on indirect bandgap materials such as silicon, the recombination of electrons and holes is non-radiative and there is no light emission. Materials used in LEDs must have a direct bandgap. Those comprised of group III and V elements of the periodic table are most common used in the fabrication of LEDs. These include GaAs and GaP. The bandgap of these materials, and hence emission wavelength, can be tailored through the addition of impurities. For instance, LEDs made solely from GaP emit green light at 555 nm. However, nitrogen-doped GaP emits at yellow-green light (565 nm), and ZnO-doped GaP emits red light (700 nm).

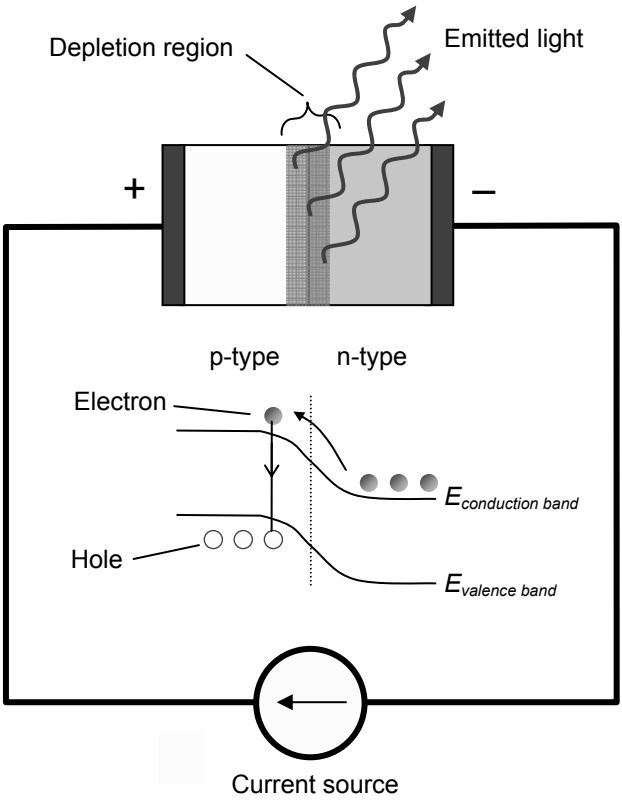

Fig. 2.12 A schematic of an LED. This band diagram illustrates the electron-hole recombination process.

The other way in which electroluminescence occurs is via the excitation of electrons using an electric field that is applied across phosphorescent materials. This type electroluminescence stems from the work of Georges Destriau[36], who in 1936 showed that by applying a large alternating potential across zinc sulfide (ZnS) phosphor powder suspended in an insulating material, electroluminescence was observed. This method for obtaining electroluminescence is the basis of current research into nanotechnology based electro luminescent displays. A typical example of such a device is seen in **Fig. 2.13**.

New *surface-conduction electron-emitter displays* (*SED*) are based on this type of electroluminescence. *Field emission display* (*FED*) is another technology which also uses phosphor coatings as the emissive medium. A FED uses a large array of fine metal tips or carbon nanotubes, with many

positioned behind each phosphor dot, to emit electrons through field emission process.

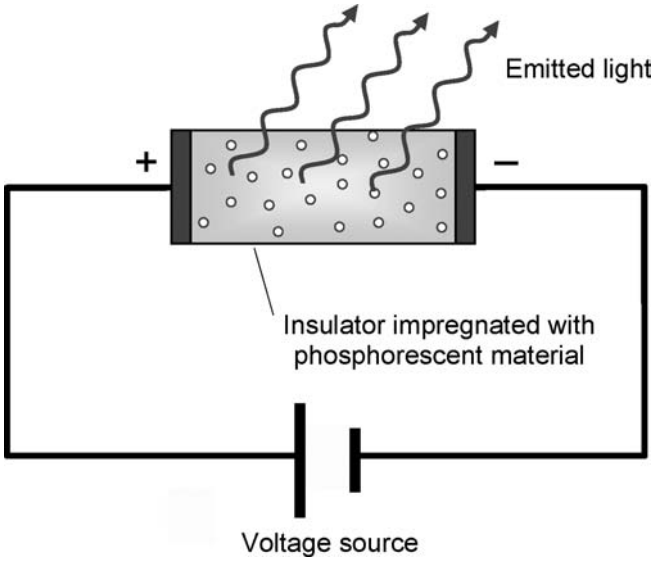

Fig. 2.13 Schematic of an electroluminescence device based on a phosphorous material.

Electroluminescent devices have many applications in chemical sensing. Example of such sensors are given by Poznyak et al.[37] They demonstrated how the electroluminescence of TiO_2 film electrodes could be utilized for measuring of hydrogen peroxide and peroxydisulphate ion concentrations in aqueous solutions. In this system, the analyte molecules are reduced on the electrode's surface, resulting in an electroluminescence whose intensity is proportional to the concentration of the measurand.

The current trend in electroluminescent device and sensor research is to utilize low dimensional nanomaterials, such as Q-dots. These nanomaterials may considerably reduce the scattering of electrons caused by defects in the bulk and reduce the non-radiative recombination rate.[38,39] They also increase in overlap of the wavefunctions for electrons and holes, and increase the electronic density of states (DOS) near the band gap of the low dimensional structures when compared with bulk materials. This leads to higher recombination rates and a narrowing of the gain spectrum.[40] As a result, LEDs incorporating low dimensional nanomaterials exhibit higher sensitivity to the applied charges. Other electroluminescence technologies include *liquid crystal display* (*LCD*), and *organic light-emitting diode*

(*OLED*), which are composed of organic thin films, such as conductive polymers are emerging.

Electroluminescent devices and sensors based on nanomaterials offer distinct advantages over those based on planar bulk materials.[41] For example, planar silicon is poorly suited to many photonic applications since it has a poor efficiency for light emission.[42] Such a deficiency can be selectively eliminated by making nanopores on the surface which provides phonon quenching or amplification capabilities. Such structures can be produced with nano-fabrication strategies, which will be discussed in the Chaps. 6 and 7.

2.3.5 Chemiluminescence Effect

Luminescence that occurs as a result of a chemical reaction is known as chemiluminescence. It is commonly observed at wavelengths from the near ultraviolet to the near infrared. Chemiluminescence can be described by the following reaction:

$$[\mathrm{A}]+[\mathrm{B}] \longrightarrow [\Diamond] \longrightarrow [\mathrm{Products}]+\mathit{light} \tag{2.11}$$

where A and B are reactants yielding an excited intermediate ◊, which is comprised of reaction products and light. Chemiluminescence has been observed for metal and semiconductor nanoparticles in chemical or electrochemical reactions.[43,44,45] When chemiluminescence takes place in living organisms, it is called *bioluminescence*.[28] Bioluminescence has emerged as an important and powerful tool in biological and medical investigations. Examples of molecules and nanomaterials that exhibit chemiluminescence employed in nanotechnology enabled sensing applications will be presented in Chaps. 6 and 7.

2.3.6 Doppler Effect

The *Doppler effect* is the apparent change in a wave's frequency as a result of the observer and the wave source moving relative to each other. If the observer and wave source are moving toward each other, the wave appears to increase in frequency and is said to be *hypsochromically* (or blue) shifted (**Fig. 2.14**). Conversely, if the wave source and observer are moving away from each other, then the wave appears to decrease in frequency and becomes *bathochromically* (or red) shifted.

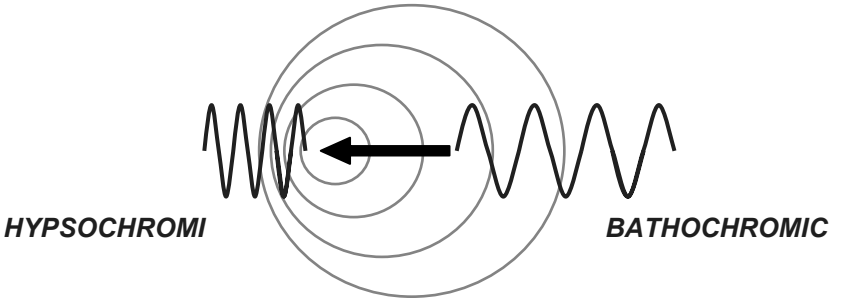

Fig. 2.14 Hypsochromic and bathochromic frequency shifts occurring as a result of the Doppler effect.

The observed Doppler shift in frequency is given by:

$$f_{observed} = \left(\frac{v}{v + v_{source}} \right) f_{source} \tag{2.12}$$

where v is the speed of the wave in the medium, v_{source} is the speed of the source with respect to the medium, and f_{source} frequency of the source wave. If the wave source approaches the observer, then v_{source} is negative, and conversely, if the wave is receding, then it takes on a positive value. A familiar examples of the Doppler effect include the changing pitch of an ambulance siren as it approaches and then drives past the observer.

Common examples of the Doppler effect in sensing include speed monitoring devices and ultrasounds. Hypsochromic and bathochromic shifts are used in measurement of large and distant bodies such as stars, galaxies and gas clouds as their motion and spectrum can be studied with respect to the observer. The Doppler effect also plays an important role in radar and sonar detection systems.

The Doppler effect can play a significant role in the sensing and characterization of nanomaterials. It is known that Doppler broadening (broadening of spectral lines in UV-vis spectroscopy) is caused by the thermal movement of small particles.[46] Doppler broadening generally places severe constraints on precise spectroscopic measurements. However, the signatures of the broadened spectrum (such as its bandwidth and shape) can be utilized to extract information about the presence of atoms/molecules in nanostructures, as well as providing information on their morphologies: by decreasing the temperature, or by employing measurement methods such

as Doppler-free saturation spectroscopy, a reference for the characterization of materials can be obtained.[47]

2.3.7 Barkhausen Effect

In 1919 Heinrich Barkhausen found that applying a slowly increasing, continuous magnetic field to a ferromagnetic material causes it to become magnetized, not continuously, but in small steps. These sudden and discontinuous changes in magnetization are a result of discrete changes in both the size and orientation of ferromagnetic domains (or of microscopic clusters of aligned atomic magnets) that occur during a continuous process of magnetization or demagnetization.

This effect generally should be reduced in the operation of magnetic sensors as it appears as a step noise in measurements. This effect is also observed in nanosized ferromagnetic materials.[48]

2.3.8 Hall Effect

Discovered in the 1880s by Edwin Hall, when a magnetic field is applied perpendicularly to the direction of an electrical current flowing in a conductor or semiconductor, an electric field arises that is perpendicular to both the direction of the current and the magnetic field. It is one of the most widely used effects in sensor technology, particularly for monitoring magnetic fields.

In **Fig. 2.15**, a magnetic field is applied perpendicularly to a thin sheet of material that is carrying a current. The magnetic field exerts a transverse force, F_B, on the moving charges and pushes them to one side. Whilst these charges build up on one side, charges of the opposite polarity build up on the other side. This charge separation creates an electric field that generates an electric force, F_E. This electric force balances the magnetic force, preventing further charge separation. As a result, there is a measurable voltage between the two sides of the material, called the Hall voltage, V_{Hall}, and is calculated using:

$$V_{Hall} = \frac{IB}{ned}, \tag{2.13}$$

where I is the current flowing through the material, B is the magnetic field, n is the charge carrier density of the material, e is the elementary electronic charge 1.602×10^{-19} C and d is the thickness of the material.

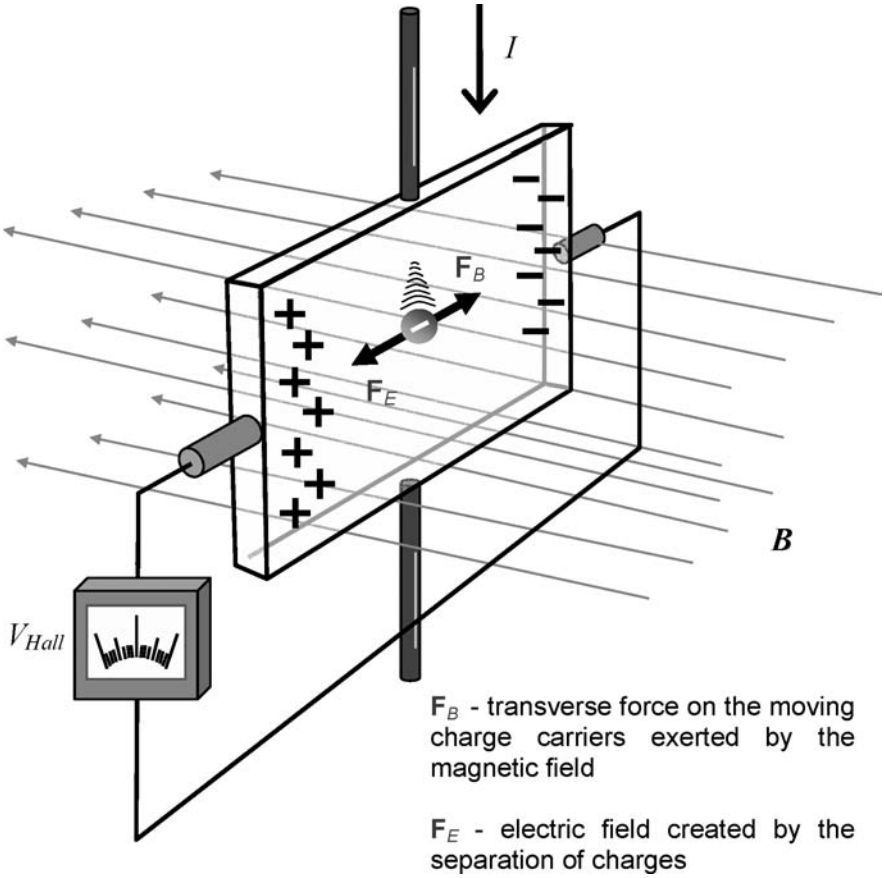

Fig. 2.15 The Hall effect.

Commercial Hall effect sensors are utilized in sensing fluid flow, power, and pressure sensing, yet they are most often employed for the measurement of magnetic fields. In fact, planar Hall sensors have been used to monitor magnetic fields in the nano-tesla range.[49] Being able to detect such low magnetic fields, the Hall effect can be implemented in the development of sensing systems which utilize nano-magnetic beads which generate very small magnetic fields. A good example of this is provide by Ejsing et al who have developed nano-magnetic bead sensors with sensitivities in the order of 3 μV/Oe mA. Their sensor response to an applied magnetic field of 250 nm magnetic beads which are commonly used for biological applications [50,51]

Spin Hall Effect

The *Spin Hall Effect* (*SHE*) refers to the generation of a spin current that is transverse to an applied electric field in such materials, resulting in an accompanying spin imbalance in the system. It occurs in paramagnetic materials as a consequence of the spin–orbit interactions. It was theoretically predicted in 1971 by Yakonov and Perel.[52] The generation, manipulation and detection of spin-polarized electrons in nanostructures are some of the current challenges of spin-based electronics.

This effect has an enormous potential to be used for sensing applications when applied to nano-magnetic beads or thin films with nano thicknesses. For instance Gerber et al[53] demonstrated that SHE can be used to sense magnetocrystalline anisotropy and magnetic moment of far-separated Co nanoparticles arranged in single-layer arrays with thicknesses as small as 0.01 nm.

2.3.9 Nernst/Ettingshausen Effect

Walther Hermann Nernst and Albert von Ettingshausen discovered that an electromotive force (e.m.f.) is produced across a conductor or semiconductor when it is subjected to both a temperature gradient and a magnetic field. The direction of the e.m.f. is mutually perpendicular to both the magnetic field and the temperature gradient. The effect can be quantified by the Nernst coefficient |N| as:

$$\left|\mathrm{N}\right| = \frac{E_Y / B_Z}{dT / dx}. \tag{2.14}$$

If the magnetic field component is in the z-direction, B_Z, then the resulting electric field component will be in the y-direction, E_Y, when subjected to a temperature gradient of dT/dx.

In spite of its potential, this effect is yet to be fully investigated for its application in nanotechnology enabled sensing. However, the authors believe this effect offers the exciting possibility of performing temperature and magnetic field strength measurements on a single nanoparticle, for example, by determining the electrical potentials across carbon nanotubes.

2.3.10 Thermoelectric (Seebeck/Peltier and Thomson) Effect

An e.m.f. is generated at the junction of two dissimilar conducting or semiconducting as a result of a temperature gradient. It was first observed in metals in 1821 by Thomas Johann Seebeck and the effect named after

him. As seen in **Fig. 2.16**, for two dissimilar materials, A and B, a voltage difference V is generated when two junctions are held at different temperatures. The voltage difference is proportional to the temperature difference, $\Delta T = T_2 - T_1$, and the relationship is given by:

$$V = (S_A - S_B)\Delta T \,, \tag{2.15}$$

where S_A and S_B are the Seebeck coefficients of material A and B, respectively. This phenomenon provides the physical basis for *thermoelements* or *thermocouples*, the standard devices for measuring temperature.

In 1834 Jean Charles Athanase Peltier found the exact opposite, observing that a temperature difference will arise at a junction of two dissimilar metals when a current is passed through them (**Fig. 2.16**). The heat per unit time, Q, absorbed by the lower temperature junction is equal to:

$$Q = (\Pi_A - \Pi_B)I \,, \tag{2.16}$$

where Π_A and Π_B are the Peltier coefficients of each material and I is the current.

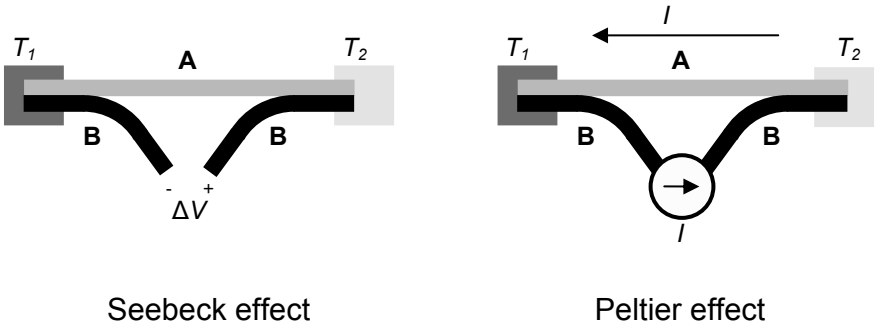

Fig. 2.16 Two dissimilar materials A and B in intimate contact, with either ends are held at different temperatures (T_1 and T_2).

William Thomson (Lord Kelvin), in 1854, discovered that an electric current flowing along a material that has a temperature gradient along its length will cause it to either absorb or release heat. The forced absorption or emission of heat is a result of energy conservation, because if a temperature gradient exists across the length of a material, an e.m.f. may be generated across this length.[5,54]

Many sensing systems incorporate temperature sensors based on the thermoelectric effect, and there are a variety of them available that find application in medical and scientific research, as well as in industrial

process control and food storage, etc. There are several types of such devices, called *thermocouples*, and among the most popular are listed in **Table 2.2**.

Table 2.2 Some common types of thermocouples.

Type	Materials	Temp. Range (ºC)
K	Chromel/Alumel (Ni-Al alloy)	−200°C to +1200
E	Chromel/Constantan	−110 to 140
J	Iron/Constantan	−40 to +750
N	Nicrosil (Ni-Cr-Si alloy)/Nisil (Ni-Si alloy)	

The different metals and alloys utilized in thermocouples result in different properties and performance. Some commonly utilized alloys are chromel (approx. 90% nickel and 10% chromium) and constantan (approx. 40% nickel and 60% copper). Type K is perhaps the most widely used thermocouple as it operates over a wide temperature range from −200 to +1200°C. This type of thermocouple has a sensitivity of approximately 41 μV/°C. Some type E thermocouples can have a narrower operating range than type K, however, their sensitivity is much higher (68 μV/°C). Type N (Nicrosil (Ni-Cr-Si alloy)/Nisil (Ni-Si alloy)) thermocouples have high stability and resistance to high temperature oxidation, making them ideal for many high temperature measurements. Other thermocouple types: B, R, and S are all made of expensive noble metals, and are the most stable for high temperature, but have low sensitivity (approximately 10 μV/°C).

Thermoelectric materials, particularly those based on semiconducting materials with large Peltier coefficients, can be used to fabricate on chip temperature sensors. [55] They are also used to make heat pumps meeting a growing demand in many products including charge coupled device (CCD) cameras, laser diodes, microprocessors, blood analyzers, etc. may employ thermoelectric coolers. The performance of thermoelectric devices in terms of the ability to convert thermal energy into electrical energy, and vice versa, depends on the *figure of merit* (*ZT*) of the material's utilized, and is given by:

$$ZT=(S^2T)/(\rho K_T), \tag{2.17}$$

where S, T, ρ and K_T are the *Seebeck coefficient*, absolute temperature, electrical resistivity and total thermal conductivity, respectively. Generally, the larger the thermoelectric material's Seebeck coefficient (to generate the maximum voltage difference) and thermal conductivity (so it does not allow the exchange of heat at two junctions), whilst lowering its elec-

trical resistivity (so the internal resistance does not generate heat), the more efficient the thermoelectric device can be.

Bismuth telluride (Bi_2Te_3) and antimony telluride (Sb_2Te_3) are semiconductor materials with high Seebeck coefficients, having *ZT* of approximately equal to unity at room temperature. In the 50s, an Australian researcher, Julian Goldsmid confirmed that bismuth telluride displays a very strong Peltier effect.[56,57] However, until only recently have crystals with higher *ZT*s have been found.

In the early 90s, it was theoretically proven that nanosized materials could dramatically enhance the performance of *Peltier modules* and devices.[58] Nanodimensional materials such as superlattices, segmented one dimensional nano-wires and zero-dimensional quantum dots are excellent candidates for development of high performance thermoelectric structures. The nano-dimensions result in confinement of the charge carriers and scattering of phonons which increase the electrical conductivity and decrease the thermal conductivity. As a result, they will have an increased value for the figure of merit. It has been calculated that for quantum wires of Bi_2Te_3 a *ZT* as large as 14 can be obtained[58,59] when the radius of wire is reduced to 0.5 nm. For a superlattice structure of the same materials with the quantum well of width of 1 nm the best calculated figure of merit is 2.5 and for a 0.5 nm quantum well it is 5.[58,59]

In a major breakthrough for the fabrication of thermoelectric superlattices, Venkatasubramanian et al.[60] reported significant enhancement in *ZT* which is almost equal to the theoretical values. They achieved a *ZT* of 2.4 for p-type Bi_2Te_3/Sb_2Te_3 superlattice devices. *ZT* of several recently reported materials has been shown in **Fig. 2.17**.

With the emergence of more efficient thermoelectric materials, in the near future, such devices may be sought for power generation and the transformation of waste thermal energy into electrical energy.

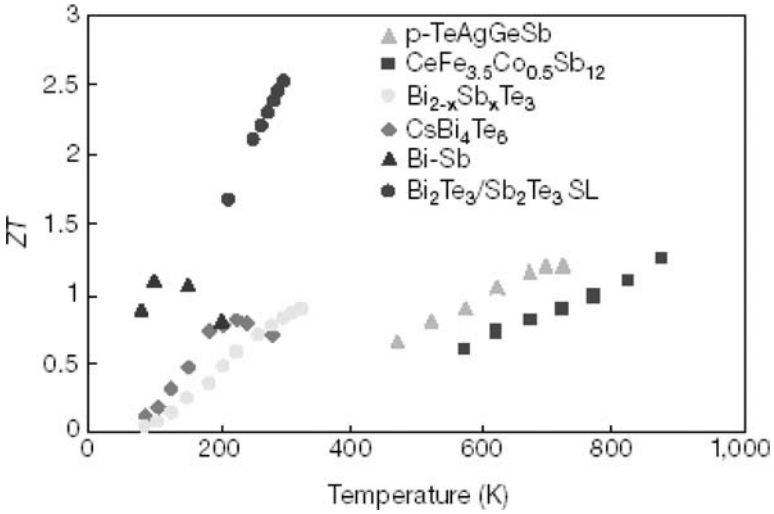

Fig. 2.17 Temperature dependence of *ZT* of 1 nm/5 nm p-type Bi_2Te_3/Sb_2Te_3 superlattice compared to those of several recently reported materials. Reprinted with permission from the Nature publications.[60]

2.3.11 Thermoresistive Effect

Thermoresistivity is concerned with the change in a material's electrical resistance with temperature and is widely used in temperature sensing applications. This effect is the basis of temperature sensing devices such as *resistance thermometers* and *thermistors*. The electrical resistance *R*, is determined by the formula:

$$R = R_{ref}\left(1 + \alpha_1 \Delta T + \alpha_2 \Delta T^2 + ... + \alpha_n \Delta T^n\right) \tag{2.18}$$

where R_{ref} is the resistance at the reference temperature, $\alpha_1 ... \alpha_n$ are the material's temperature coefficient of resistance, $\Delta T = (T\text{-}T_{ref})$ is the difference between the current temperature *T* and the reference temperature T_{ref}. The equation suggests that resistance increases with temperature. This is not the case for all materials, for if the material has a *positive temperature coefficient* (*PTC*) then its resistance increases with temperature, conversly if it has a *negative temperature coefficient* (*NTC*),) then it decreases.

In many cases, materials exhibit a linear relationship between the temperature and resistance, and hence the higher order terms in Eq. (2.18) can

be disregarded. However, this linearity is valid only for a limited range of temperatures (**Table 2.3**).

Table 2.3 The temperature range of some metals used as thermoresistive based temperature sensors.

Material	Linear temperature range (°C)
Copper	–200–260
Platinum	–260–1000

Nanomaterials can be implemented for the fabrication of thermistors with desired positive and negative temperature coefficients. Additionally, in conventional materials only the surface of the bulk or thin films is exposed to the environmental changes such as ambient temperature alterations. However, nanostructured materials with a larger surface to volume ratio are more efficiently exposed to the environmental changes. This both increases the sensor response magnitude and reduces its response time.

For instance, Saha et al[61] successfully prepared nano-size powders of $(Mn_xFe_{1-x})_2O_3$ by citrate–nitrate gel method with sintering at high temperature of 1500°C. The developed materials were found to have NTC sensitivity index (β- the measure of sensitivity for a thermoresistive material) as high as 6000 K (in the temperature range of 50–150°C) which is appreciably higher than that of conventional NTC materials. The electrical characteristics of conductive/nonconductive polymer composites mixed with nano-sized particles can also be utilized for the fabrication of thermistors.[62]

2.3.12 Piezoresistive Effect

The piezoresistive effect describes the change in a material's electrical resistivity when acted upon by a mechanical force. This effect takes its name from the Greek word *piezein*, which means to squeeze. It was first discovered in 1856 by Lord Kelvin who found that the resistivity of certain metals changed when a mechanical load was applied. Piezoresitance can be described by the following equation for semiconductors:

$$\frac{\Delta R}{R} = \pi\sigma, \tag{2.19}$$

where π is the *tensor element of the piezoresistive coefficient*, σ is the mechanical stress tensor, and R and ΔR are the resistance and the change in resistance, respectively.

In 1954, C. S. Smith[63] discovered that semiconductors such as silicon and germanium displayed a much greater piezoresistive effect than metals.

There are two phenomena attributed to silicon's resistivity changes: the stress dependent distortion of its geometry; and the stress dependence of its resistivity.

The piezoresistive effect in semiconductors and metal alloys is exploited in sensors. Most materials exhibit some piezoresistive effect. However, as silicon is the material of choice for integrated circuits, the use of piezoresistive silicon devices, for mechanical stress measurements, has been of great interest.[64] The most widely used form of piezoresistive silicon based sensors are diffused resistors.[65] The effect also can be used in cantilever based sensors.[66]

The effects of stress are far more significant on crystalline materials' with nanometer thick planes than they are on bulk materials. For example, for one and two dimensional nanomaterials, the effect of an external force is limited in one and two dimensions which confine the movement of phonons. Additionally for nanomaterials the area for which the external force can act on is greatly reduced. As a result, the effective force per area (i.e. stress), is amplified. Therefore, stress acting on a nanocrystal of a piezoresistive material can be translated into a large change in the crystal's conductivity.

Nanosized piezoresitive elements are developed for both chemical and physical sensing applications. The major advantage of such systems is the ease of measurement, which is basically a voltage or current. A fine example of such sensors is demonstrated in the work by Stampfer et al.[67] They reported the fabrication and characterization of pressure sensors based on individual single-walled carbon nanotubes (SNWT) as electromechanical transducing elements. Their sensor consists of an individual electrically connected SWNT adsorbed on top of a 100-nm-thick atomic layer deposited circular alumina (Al_2O_3) membrane with a radius in the range of 50-100 μm. They performed electromechanical measurements on strained metallic SWNTs adhering to this membrane and found a piezoresistive gauge factor of approximately 210 for SWNTs. The fabrication process of such a device is shown in **Fig. 2.18**. The schematic of such a device is shown in **Fig. 2.19**.

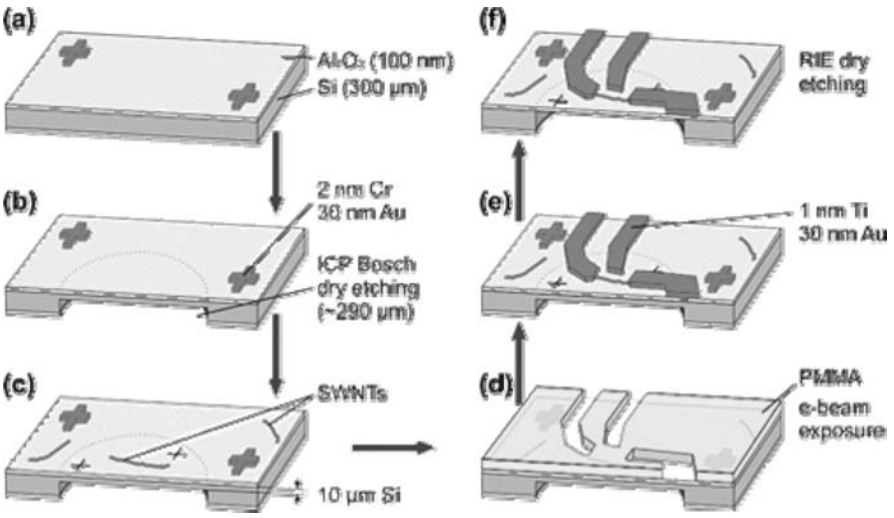

Fig. 2.18 Process flow to fabricate single-walled-carbon-nanotube-based pressure sensors: (a) 100 nm of Al_2O_3 is deposited by atomic layer deposition on a 300-µm-thick Si substrate. Photolithography and lift-off processes are used for patterning. (b) The membrane openings are patterned using infrared backside alignment and anisotropically dry etched from the backside. (c) SWNTs are dispersed from a solution onto the Al_2O_3. (d) PMMA (a polymer) spin coating and e-beam exposure. (e) Metalization and lift-off to electrically connect the SWNTs, and the final dry etch membrane release (f). Reprinted with permission from the American Chemical Society publications.[67]

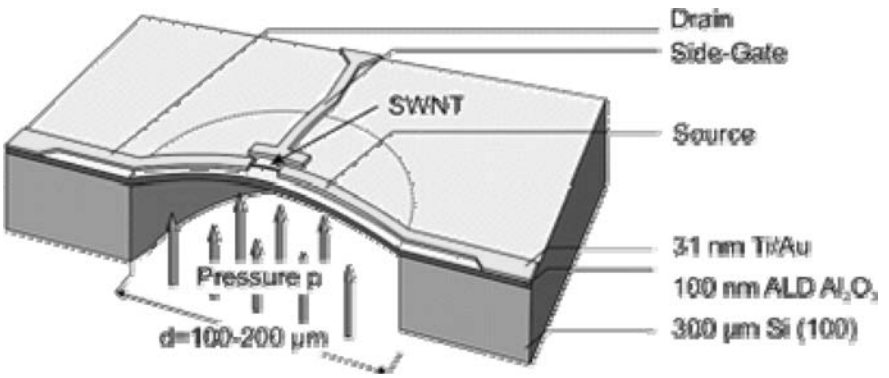

Fig. 2.19 Schematic of the SWNT based piezoresistive device. Reprinted with permission from the American Chemical Society publications.[67]

2.3.13 Piezoelectric Effect

Piezoelectricity is the ability of crystals that lack a centre of symmetry to produce a voltage in response to an applied mechanical force, and vice versa (**Fig. 2.20**). It was discovered by the Curie brothers in 1880.

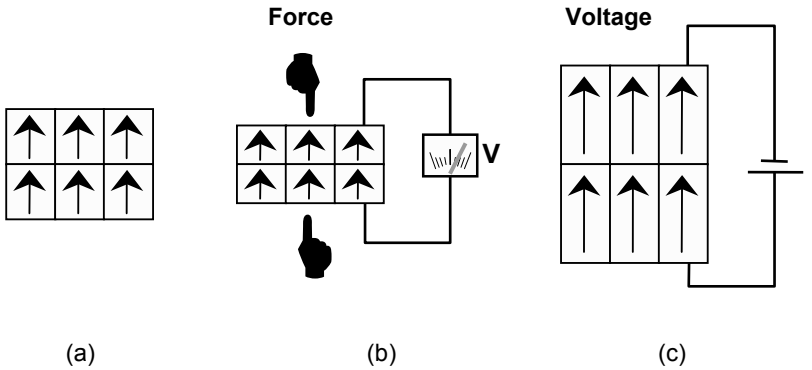

Fig. 2.20 (a) A piezoelectric material. (b) A voltage response can be measured as a result of a compression or expansion. (c) An applied voltage expands or compresses a piezoelectric material.

Out of thirty-two crystal classes, twenty-one do not have a centre of symmetry (non-centro-symmetric), and of these, twenty directly exhibit piezoelectricity (except the cubic class 432). The most popular piezoelectric materials are quartz, lithium niobate, lithium tantalite, PZT and langasite. Many piezoelectric materials are ferroelectric ceramics, which become piezoelectric when poled with an external electric field (**Fig. 2.21**). Piezoelectric crystallites are centro-symmetric cubic (isotropic) before poling and after poling exhibit tetragonal symmetry (anisotropic structure) below the Curie temperature. Above this temperature they lose their piezoelectric properties.

Polymers such as rubber, wool, hair, wood fiber and silk also exhibit piezoelectricity to some extent. Polyvinylidene fluoride (PVDF) is a thermoplastic material that when poled exhibits piezoelectricity several times greater than quartz.

Piezoelectric materials are an extremely popular choice for a broad variety of sensing applications. In Chap. 3, several transducers exploiting the piezoelectric effect will be presented and examples of piezoelectric materials employed in nanotechnology enabled sensing applications will be given in Chaps. 6 and 7.

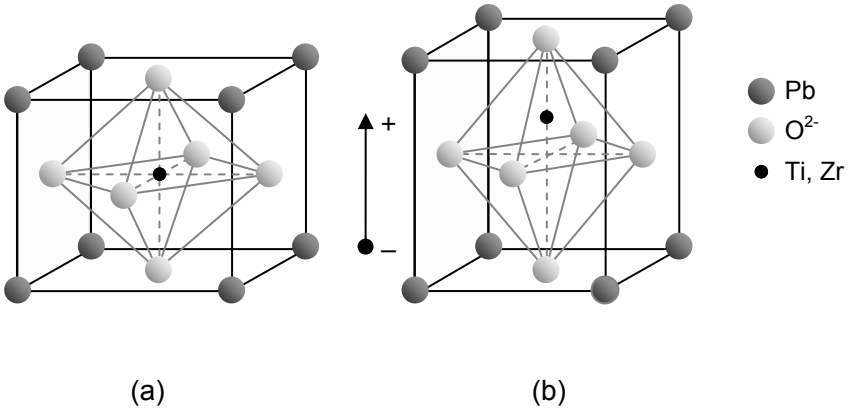

Fig. 2.21 A schematic of piezoelectricity in a PZT crystal: (a) before poling (b) after poling.

2.3.14 Pyroelectric effect

When heated or cooled, certain crystals establish an electric polarization, and hence generate an electric potential. The temperature change causes positive and negative charges to migrate to the opposite ends of a crystal's polar axis. Such polar crystals are said to exhibit *pyroelectricity*, which takes its name from the Greek word *pyro* which means fire.

The pyroelectric materials are employed in radiation sensors, in which radiation incident on their surface is converted to heat. The increase in temperature associated with this incident radiation causes a change in the magnitude of the crystal's electrical polarization. This results in a measurable voltage, or if placed in a circuit, a measurable current given by:

$$I = pA\frac{dT}{dt}, \tag{2.20}$$

where p is the pyroelectric coefficient, A is the area of the electrode and dT/dt is the temperature rate of change.

Pyroelectric effect can be used to generate strong electric fields (giga-V/m) in some materials, by heating them from −30°C to +45°C in a few minutes. Researchers at UCLA headed by Brian Naranjo, recently observed the nuclear fusion of deuterium nuclei in a tabletop device.[68]

Irradiation sensors based on the pyroelectric effect are commercially available, such sensors respond to a wide range of wavelengths. Pyroelectric

sensors, which are fabricated from pyroelectric materials such as lithium tantalate and PZT, generate electric charges with small temperature changes caused by irradiation of the surface of the crystal.[69]

Most of the measurement standards for radiometry are based on thermal detectors. These devices employ some form of thermal-absorber coating such as carbon-based paint or diffuse metals such as gold.[70] Potentially, coatings with nanomaterials present an alternative to these technologies which provides higher sensitivity for measurements.[70]

It is possible to increase the pyroelectric coefficient of polymers by adding nano-particles. Zhang et al[71] showed that nanocrystalline calcium and lanthanum powder incorporated into a polyvinylidene fluoride-trifluoroethylene [P(VDF-TrFE)] copolymer matrix have a higher pyroelectric coefficient (by ~35%) than those of the P(VDF-TrFE) film of a similar thickness. It is also possible to indirectly use nanomaterials to enhance the performance of pyroelectric sensors. For instance, Liang et al[72] uatlized porous SiO_2 film as a thermal-insulation layer to block the diffusion of heat flow from the pyroelectric layer to the silicon substrate in multilayer pyroelectric thin film IR detector. This improves the energy confinement within the pyroelectric sensing layer, resulting in an enhanced performance of the sensor.

2.3.15 Magneto-Mechanical Effect (Magnetostriction)

Magnetostriction, also called the *magneto-mechanical effect*, is the change in a material's dimensions when subjected to an applied magnetic field, or alternatively it is a change in a material's magnetic properties under the influence of stress and strain. It was first identified in 1842 by James Joule while examining a sample of nickel. Its name originates from the Greek word, *magnet* and the Latin word *strictus* (meaning compressed, pressured, tense).

The mechanism that occurs in magnetostriction is illustrated in **Fig. 2.22**. As can be seen, the domains arrange themselves randomly in a non-magnetized material. Upon magnetizing, the material's domains orient with their axes which changes the length of the structure.

Magnetostrictive materials convert magnetic energy into kinetic energy, and vice versa. Therefore, they are regularly used for sensing and actuation. Interestingly, this effect causes the familiar humming sound that is heard in electrical transformers.

Magnetostriction is defined by the magnetostrictive coefficient, Λ. It is defined as the fractional change in length as the magnetization of the material increases from zero to the saturation value. The coefficient, which is

typically in the order of 10^{-5}, can be either positive or negative. The reciprocal of this effect is called the *Villari effect*, where a material's susceptibility changes when subjected to a mechanical stress.

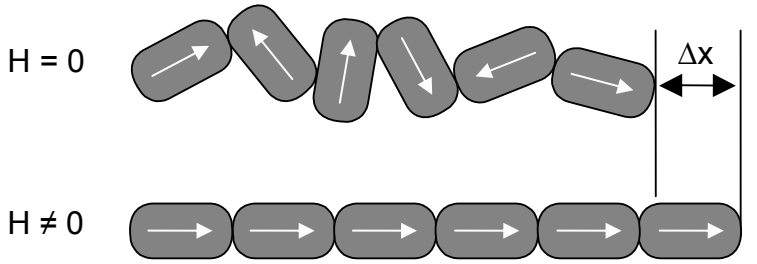

Fig. 2.22 A schematic of the Magnetostriction effect: un-aligned magnetic domains (*top*) will align causing the structure to expand under the influence of an applied magnetic field (*bottom*).

Magnetostriction is defined by the magnetostrictive coefficient, Λ. It is defined as the fractional change in length as the magnetization of the material increases from zero to the saturation value. The coefficient, which is typically in the order of 10^{-5}, can be either positive or negative. The reciprocal of this effect is called the *Villari effect*, where a material's susceptibility changes when subjected to a mechanical stress.

An element of the periodic table that exhibits the largest room temperature magnetostriction is cobalt. However, the most advanced magnetostrictive materials, called *Giant Magnetostrictive* (*GM*) materials, are alloys composed of iron (Fe), dysprosium (Dy) and terbium (Tb). Many of which were discovered at Naval Ordnance Lab and Ames Laboratory in mid 1960s.[73] Their Λ values can be three orders of magnitude larger than those of pure elements. The GM effect can be used in the development of magnetic field, current, proximity and stress sensors.[74]

2.3.16 Mangnetoresistive Effect

Magnetoresistance is the dependence of a material's electrical resistance on an externally applied magnetic field. The applied magnetic field causes a Lorentz force to act on the moving charge carriers, and depending on the field's orientation, it may result in a resistance to their flow. It was first observed by Lord Kelvin in 1856. The effect has become much more

prominent owing to the discoveries of *anisotropic magnetoresistance* (*AMR*) [75] and *giant magnetoresistance* (*GMR*) .[76]

AMR is an effect that is only found in ferromagnetic materials, where the electrical resistance increases when the direction of current is parallel to the applied magnetic field. The change in the material's electrical resistivity depends on the angle between the directions of the current and the ferromagnetic material's magnetization. It is possible to develop sensors for monitoring the orientation of magnetic fields based on the AMR effect. In these sensors, the resistance changes when the current parallel to the magnetic moment alters or passes near the magnetic field. However, the resistance change associated with AMR effect is quite small and typically only of the order of one or two percent.

GMR is playing a significant role in nanotechnology enabled sensing. It was first discovered independently in 1988 by research teams led by Peter Grünberg[77] of the Jülich Research Centre and Albert Fert[76] of the University of Paris-Sud. It relies on the quantum nature of materials, and is mostly observed in layered structures that are composed of alternating ferromagnetic and nonmagnetic metal layers, with the thickness of the nonmagnetic layer being a nanometer or so. The effect is illustrated in **Fig. 2.23**. Electron scattering at the ferromagnetic/nonmagnetic interfaces depends on the whether the electron spin is parallel or antiparallel to the magnetic moment of the layer. An electron has two spin values; up and down. The first magnetic layer allows electrons in only one spin state to pass through easily. If the magnetic moments of the adjacent layers are aligned, then only electrons with that matching spin value can easily pass through the structure, and the resistance is low. If the magnetic moments of the adjacent layers are not aligned, then electrons with mismatching spin cannot pass through the structure easily and the electrical resistance is much greater than when the alignments are parallel.

The GMR effect can be utilized to monitor magnetic fields, for in the presence of an applied magnetic field, the relative orientations of the magnetic moments in the alternating ferromagnetic layers change and hence a change in resistance is observed. Currently, research is focused on employing multilayered nanowires (which offer greater sensitivity than the thin films now used in hard drives' reader/writers), which also exhibit GMR. It is largely used in read heads of the magnetic discs for computers information storage for sensing magnetic fields, among other sensing applications.[78] Further sensing examples utilizing this effect will be presented in Chap. 7.

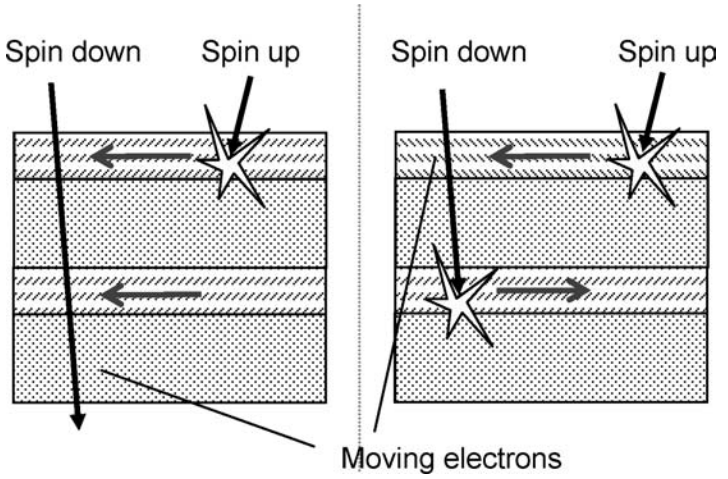

Fig. 2.23 A schematic of the GMR effect after and before applying the magnetic field.

2.3.17 Faraday-Henry Law

The Faraday-Henry law is a fundamental law of electromagnetism, and expresses that an electric field is induced by changing the magnetic field (**Fig. 2.24**). Michael Faraday and Joseph Henry both independently discovered the electromagnetic phenomenon of self and mutual inductance. Their work on the magnetically induced currents was the basis of the electrical telegraph, which was jointly invented by Samuel Morse and Charles Wheatstone later on. Early acoustic sensors and devices (such as microphones), analogue current/voltage meters, and reed-relay switches make use of this effect.

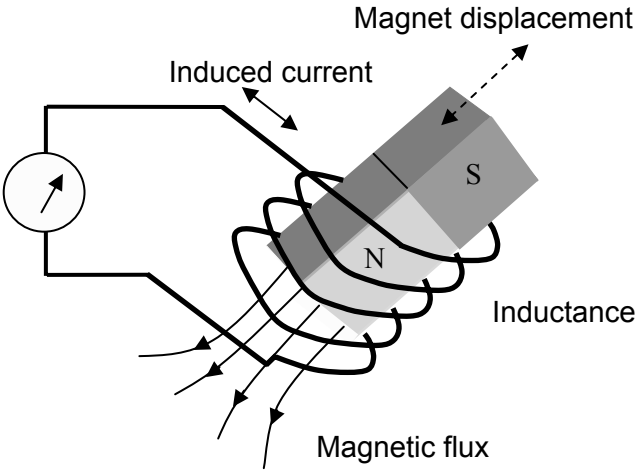

Fig. 2.24 A schematic of the Faraday-Henry effect.

The relation between the electric field, **E**, and the magnetic flux density, **B**, is defined by:

$$\oint_C \mathbf{E} \cdot d\mathbf{s} = -\frac{d}{dt} \oint_S \mathbf{B} \cdot dA \,, \tag{2.21}$$

or in differential form:

$$\nabla \times \mathbf{E} = -\frac{\partial \mathbf{B}}{\partial t} \,, \tag{2.22}$$

This law governs antennas, electrical motors and a large number of electrical devices that include relays and inductors in telecommunication circuits. Almost all *radio frequency identification* (*RFID*) tags and sensing systems, which are currently used in warehouses, are based on the Faraday-Henry effect. Such tags are commonly used in supermarkets, shops and offices for identifying the products, improving inventory and logistical efficiency.

Researchers have developed relay switches and actuators based on carbon nanotubes.[79] Such actuators can be used as sensing templates by functionalizing regions with sensitive elements. A conceptual drawing and SEM image of the nanoactuator has been shown in **Fig. 2.25** . As can be seen, a metal plate rotor (R) is attached to a multi-walled carbon nanotube (*MWCNT*) which acts as a support shaft and is the source of rotational

freedom. Electrical contact to the rotor plate is made via the MWCNT and its anchor pads (A1, A2). Three stator electrodes, two on the SiO_2 surface (S1, S2) and one buried beneath the surface (S3), provide additional voltage control elements. The SiO_2 surface has been etched down to provide full rotational freedom for the rotor plate. The entire actuator assembly is integrated on a Si chip. A scanning electron microscope (SEM) image of nanoactuator is also shown.

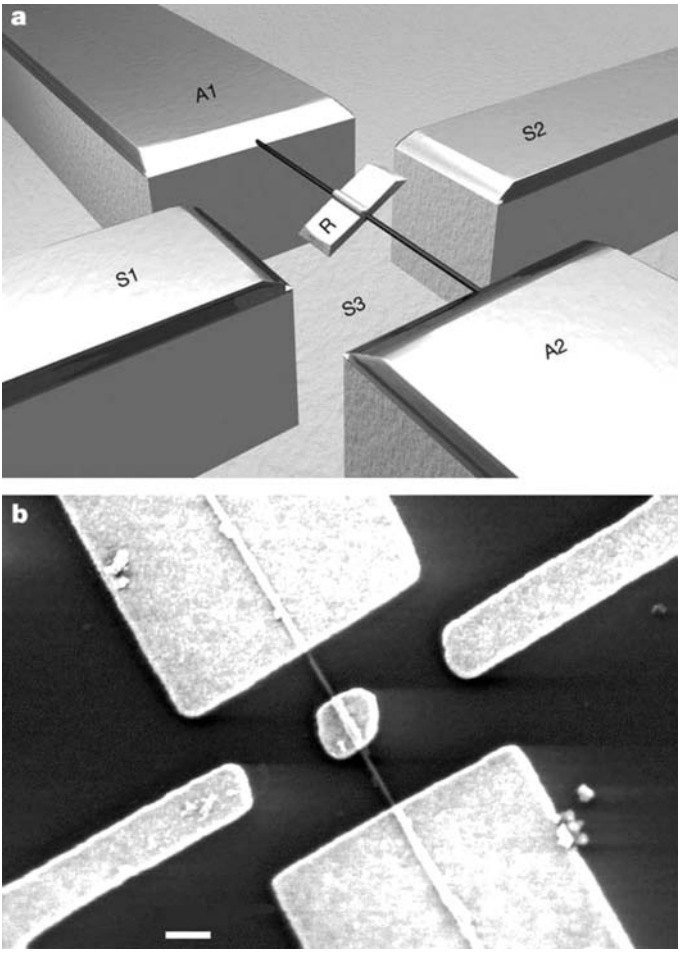

Fig. 2.25 (top) Conceptual drawing and SEM image of the nanoactuator. (bottom) Scanning electron microscopy. The scale bar is 300 nm. Reprinted with permission from the Nature publications.[79]

2.3.18 Faraday Rotation Effect

Discovered by Michael Faraday in 1845, it is a magneto-optic effect in which the polarization plane of an electromagnetic wave propagating through a material becomes rotated when subjected to a magnetic field that is parallel to the propagation direction. This rotation of the polarization plane is proportional to the intensity of the applied magnetic field. This effect was the first experimental evidence that light is an electromagnetic wave and was one of the foundations on which James Clerk Maxwell developed his theories on electromagnetism. The angle of rotation is defined by the equation:

$$\theta = \mathrm{V}\mathbf{B}l\,, \tag{2.23}$$

where **B** is the magnetic flux density, V is the *Verdet constant* and l is the length of the material through which the light is passing.

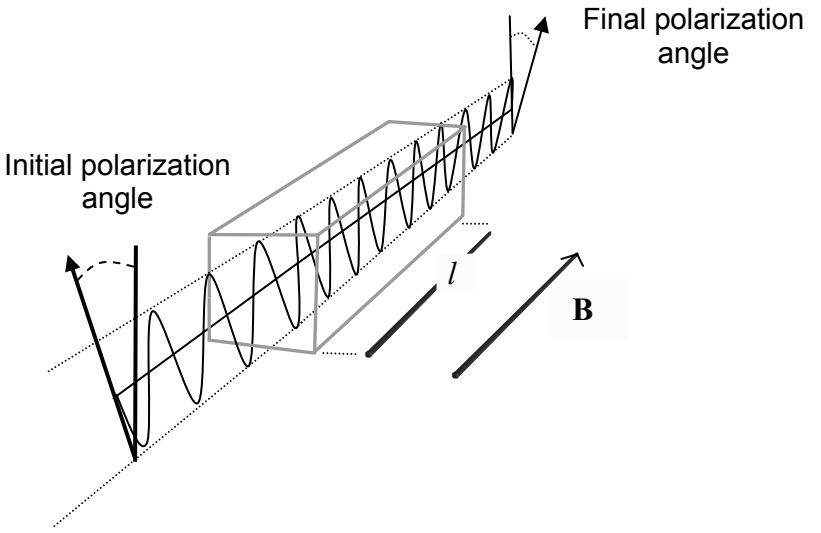

Fig. 2.26 A schematic of the Faraday effect: rotation of the polarization plane as a result of an external magnetic field.

As the polarized beam enters the material, *birefringence* occurs, in which the wavefront is split into two circularly polarized rays. This is caused when the light travels parallel to the magnetic field lines, the absorption line splits into two components which are circularly polarized in opposite directions. This is the *Zeeman effect*, where the splitting of spectral lines into multiple components in a magnetic field is produced. These

circularly polarized waves will propagate at different velocities due to the difference in the refractive indices of the two rays. As the rays emerge from the material, they will recombine. However, owing to the changes in the difference in propagation speed, and hence refractive indices, the recombined wave will possess a net phase offset which will result in a rotation of the angle of linear polarization.

Most substances do not show such a difference without an external magnetic field, except optically active substances such as crystalline quartz or a sugar solution. Also, the refractive index in the vicinity of an absorption line does changes with frequency.

There are several applications of Faraday rotation in measuring instruments. For instance, it has been used to measure optical rotatory power,[80] for amplitude modulation of light, and for remote sensing of magnetic fields.[81]

The Verdet constant is a figure of merit used to compare this effect between materials, and has units of angular rotation per unit of applied field per unit of material length.[82] A common magneto-optical material for field sensing is terbium gallium garnet, which has a Verdet constant of 0.5 min/(G cm). Along with a relatively high Verdet constant, this material also can take on a permanent magnetization. It is possible to construct magneto-optical magnetometers with a sensitivity of 30 pT for the detection of magnetic nano-beads for sensing applications. The unique advantage that the magneto-optical sensor has over other magnetic sensors is its quick response time. Sensors with gigahertz responses have been fabricated.[82]

2.3.19 Magneto-Optic Kerr Effect (MOKE)

In 1877, John Kerr discovered that the polarization plane of a light beam incident on a magnetized surface is rotated by a small amount after it is reflected from that surface. This is because the incoming electric field, E, exerts a force, F, on the electrons in the material, and consequently they vibrate in the plane of polarization of the incoming wave. If the material has some magnetization, M, then the reflected wave gain a small electric field component (called the Kerr component, K),[83] as seen in **Fig. 2.27**. As a result, the reflected wave is rotated with respect to the incident wave. The amount of rotation depends on the magnitude of M.[84,85] Both the magneto-optic Kerr and Faraday rotation effects occur because the magnetization in the material produces a change its dielectric tensor.

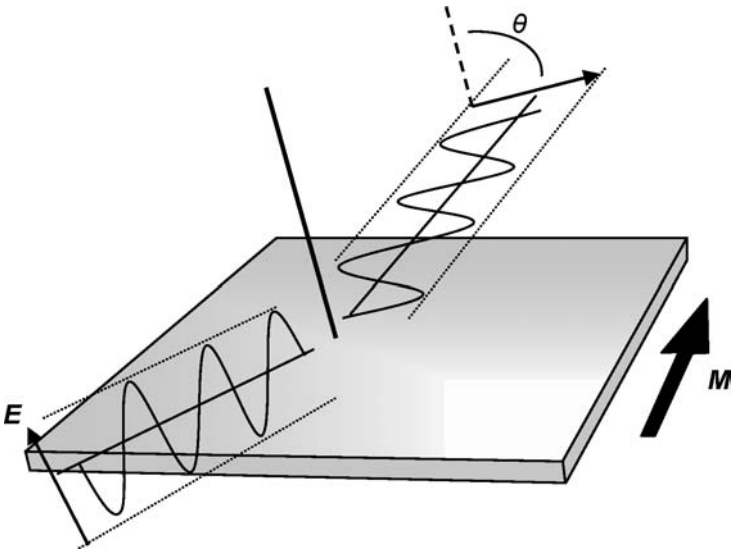

Fig. 2.27 Rotation of the polarization plane on a magnetized surface as a result of the magneto-optic Kerr effect.

The Kerr effect can be used to fabricate sensors for various applications**.** For instance, Karl et al [86] developed a pressure sensor based on a micromembrane coated with a magnetostrictive thin-film. The pressure difference across the diaphragm causes deflection and thus stress in the magnetostrictive layer. This leads to a change in the magnetic properties of the thin-film, which can be measured as a change in the MOKE properties. It is widely utilized for determining the magnetization of materials. MOKE can also be used to study the magnetic anisotropy of deposited ferromagnetic thin films. Magnetic properties of such films are closely related to their morphology and micro/nano structures. [87]

2.3.20 Kerrand Pockels Effects

Discovered by John Kerr in 1875, it is an electro-optic effect in which a material changes its refractive index in response to an electric field. Here, birefringence is induced electrically in isotropic materials.[88] When an electric field is applied to a liquid or a gas, its molecules (which have electric dipoles) may become partly oriented with the field.[5] This renders the substance anisotropic and causes birefringence in the light traveling through it. However, only light passing through the medium normal to the electric

field lines experience such birefringence, and it is proportional to the square of the electric field. The amount of birefringence due to the Kerr effect can be given by:

$$\Delta n = n_o - n_e = \lambda_o K E^2 , \tag{2.24}$$

where E is the electric field strength, K is the Kerr-Pockels constant and λ_o is the wavelength of free space. The two principal indices of refraction, n_o and n_e are the ordinary and extraordinary indices, respectively. The effect is utilized in many optical devices such as switches and monochromators, modulators. This effect is analogous to the Faraday effect but for electric fields.

Pockels effect is a similar effect to the Kerr effect, with differences of the birefringence being directly proportional to the electric field, not its square (as in the Kerr effect). Only crystals that lack a center of symmetry (20 out of the 32 classes) may show this effect.

Optical sensors based on the Pockels effect are being implemented in industrial applications. Pockels voltage sensors have been incorporated into electric power networks and power apparatus such as gas-insulated-switchgear. Pockels field sensors are applied to the measurement of not only the electrostatic field but also the space charge field in electrical discharges subjected to dc, ac, lightning impulse, or switching impulse voltages.[89]

2.4 Summary

The terminology and parameters frequently encountered in sensing were presented in this chapter. In addition, some of the most widely utilized physical effects for signal transduction related to nanotechnology enabled sensors were introduced. Several examples of nanomaterials exhibiting these effects were also provided. It was shown that these effects became dramatically enhanced by the use of nanomaterials. It should be noted that many other effects are also known and widely employed in sensing, yet are not commonly utilized in nanotechnology enabled sensing applications. However, novel nanotechnology enabled sensors are emerging rapidly, and effects previously believed to be irrelevant are finding acceptance and novel applications.

In next chapter, several transduction platforms that are used in conjunction with nanostructured materials for nanotechnology enabled sensing will be introduced.

References

[1] W. Göpel, J. Hesse, and J. N. Zemel, *Sensors: A Comprehensive Survey* (VCH, Weinheim, Germany, 1991).

[2] M. J. Usher and D. A. Keating, *Sensors and transducers: characteristics, applications, instrumentation, interfacing* (Macmillan, London, UK, 1996).

[3] R. Pallas-Areny and J. G. Webster, *Sensors and Signal Conditioning* (Wiley, New York, USA, 1991).

[4] H. Lin, T. Jin, A. Dmytruk, M. Saito, and T. Yazawa, Journal of Photochemistry and Photobiology a-Chemistry **164,** 173-177 (2004).

[5] J. Daintith, *A Dictionary of Physics.* (Oxford University Press, London, UK, 2000).

[6] R. Calarco, M. Marso, T. Richter, A. I. Aykanat, R. Meijers, A. V. Hart, T. Stoica, and H. Luth, Nano Letters **5,** 981-984 (2005).

[7] M. C. Beard, G. M. Turner, and C. A. Schmuttenmaer, Nano Letters **2,** 983-987 (2002).

[8] F. A. Hegmann, R. R. Tykwinski, K. P. H. Lui, J. E. Bullock, and J. E. Anthony, Physical Review Letters **89** (2002).

[9] R. W. Miles, K. M. Hynes, and I. Forbes, Progress in Crystal Growth and Characterization of Materials **51,** 1-42 (2005).

[10] A. S. Achoyan, A. E. Yesayan, E. M. Kazaryan, and S. G. Petrosyan, Semiconductors **36,** 903-907 (2002).

[11] N. Tsutsui, V. Ryzhii, I. Khmyrova, P. O. Vaccaro, H. Taniyama, and T. Aida, Ieee Journal of Quantum Electronics **37,** 830-836 (2001).

[12] V. M. Aroutionian, S. G. Petrosyan, and A. E. Yesayan, Thin Solid Films **451-52,** 389-392 (2004).

[13] R. P. Raffaelle, B. J. Landi, J. D. Harris, S. G. Bailey, and A. F. Hepp, Materials Science and Engineering B-Solid State Materials for Advanced Technology **116,** 233-243 (2005).

[14] T. J. Bukowski and J. H. Simmons, Critical Reviews in Solid State and Materials Sciences **27,** 119-142 (2002).

[15] G. Khrypunov, A. Romeo, F. Kurdesau, D. L. Batzner, H. Zogg, and A. N. Tiwari, Solar Energy Materials and Solar Cells **90,** 664-677 (2006).

[16] J. R. Sites and X. X. Liu, Solar Energy Materials and Solar Cells **41-2,** 373-379 (1996).

[17] F. Kessler, D. Herrmann, and M. Powalla, Thin Solid Films **480,** 491-498 (2005).

[18] A. G. MacDiarmid, Synthetic Metals **125,** 11-22 (2001).

[19] A. G. MacDiarmid, Reviews of Modern Physics **73,** 701-712 (2001).

[20] A. G. MacDiarmid and A. J. Epstein, Makromolekulare Chemie-Macromolecular Symposia **51,** 11-28 (1991).
[21] W. U. Huynh, J. J. Dittmer, and A. P. Alivisatos, Science **295,** 2425-2427 (2002).
[22] B. Oregan and M. Gratzel, Nature **353,** 737-740 (1991).
[23] C. B. Cohen and S. G. Weber, Analytical Chemistry **65,** 169-175 (1993).
[24] J. P. Spoonhower, Photographic Science and Engineering **24,** 130 (1980).
[25] R. Janes, M. Edge, J. Robinson, J. Rigby, and N. Allen, Journal of Photochemistry and Photobiology a-Chemistry **127,** 111-115 (1999).
[26] E. N. Harvey, *A History of Luminescence* (American Philosophical Society, Philadelphia, USA, 1957).
[27] B. J. Clark, T. Frost, and M. A. Russell, *UV spectroscopy : techniques, instrumentation, data handling* (Chapman & Hall, London, UK, 1993).
[28] N. W. Barnett and P. S. Francis, in *Encyclopedia of Analytical Science*, edited by C. F. Poole, A. Townshend, and P. J. Worsfold (Academic Press, New York, USA, 2004), p. 305-315.
[29] G. Blasse and B. C. Grabmaier, *Luminescent Materials* (Springer-Verlag, New York, USA, 1995).
[30] T. H. Gfroerer, in *Encyclopedia of Analytical Chemistry*, edited by R. A. Meyers (John Wiley & Sons Ltd., Chichester, UK, 2000), p. 9209-9231.
[31] R. Weissleder, C. H. Tung, U. Mahmood, and A. Bogdanov, Nature Biotechnology **17,** 375-378 (1999).
[32] A. P. Alivisatos, Science **271,** 933-937 (1996).
[33] P. N. Prasad, *Introduction to Biophotonics,* (Wiley Interscience, Hoboken, USA, 2003).
[34] C. Seydel, Science **300,** 80-81 (2003).
[35] W. C. W. Chan and S. M. Nie, Science **281,** 2016-2018 (1998).
[36] G. Destriau, Journal de Chemie Physique **33,** 587-625 (1936).
[37] S. K. Poznyak and A. I. Kulak, Talanta **43,** 1607-1613 (1996).
[38] D. Huang, M. A. Reshchikov, and H. Morkoc, in *Quantum Dots*, edited by E. Borovitskaya and M. S. Shur (World Scientific, Singapore, 2002), p. 79.
[39] E. Borovitskaya and M. S. Shur, in *Quantum Dots*, edited by E. Borovitskaya and M. S. Shur (World Scientific, Singapore, 2002), p. 1.
[40] G. B. Stringfellow, in *High brightness light emitting diodes* (Academic Press, San Diego, USA, 1997).

[41] Y. Huang, X. F. Duan, and C. M. Lieber, Small **1,** 142-147 (2005).
[42] P. H. Zhang, V. H. Crespi, E. Chang, S. G. Louie, and M. L. Cohen, Nature **409,** 69-71 (2001).
[43] S. K. Poznyak, D. V. Talapin, E. V. Shevchenko, and H. Weller, Nano Letters **4,** 693-698 (2004).
[44] H. Cui, Z. F. Zhang, and M. J. Shi, Journal of Physical Chemistry B **109,** 3099-3103 (2005).
[45] G.-F. Jie, B. Liu, J.-J. Miao, and J.-J. Zhu, Talanta (2006).
[46] P. J. Chantry, Journal of Chemical Physics **55,** 2746& (1971).
[47] E. S. Polzik, J. Carri, and H. J. Kimble, Physical Review Letters **68,** 3020-3023 (1992).
[48] A. Zhukov, J. Gonzalez, J. M. Blanco, M. Vazquez, and V. Larin, Journal of Materials Research **15,** 2107-2113 (2000).
[49] F. N. Van Dau, A. Schuhl, J. R. Childress, and M. Sussiau, Sensors and Actuators A **53,** 256-260 (1996).
[50] L. Ejsing, M. F. Hansen, A. K. Menon, H. A. Ferreira, D. L. Graham, and P. P. Freitas, Journal of Magnetism and Magnetic Materials **293,** 677-684 (2005).
[51] L. Ejsing, M. F. Hansen, A. K. Menon, H. A. Ferreira, D. L. Graham, and P. P. Freitas, Applied Physics Letters **84,** 4729-4731 (2004).
[52] M. I. Dyakonov and V. I. Perel, Physical Letters A **35,** 459-460 (1971).
[53] A. Gerber, A. Milner, J. Tuaillon-Combes, M. Negrier, O. Boisron, P. Melinon, and A. Perez, Journal of Magnetism and Magnetic Materials **241,** 340-344 (2002).
[54] M. W. Zemansky and R. H. Dittman, *Heat and thermodynamics: an intermediate textbook*, 6th ed. (McGraw-Hill, New York, USA, 1981).
[55] H. Baltes, O. Paul, and O. Brand, Proceedings of the IEEE **86,** 1660 - 1678 (1998).
[56] H. J. Goldsmid, *Thermoelectric Refrigeration* (Plenum, New York, USA, 1964).
[57] H. J. Goldsmid and G. S. Nolas, in *A review of the New Thermoelectric Materials*, 2001, p. 1-6.
[58] L. D. Hicks and M. S. Dresselhaus, Physical Review B **47,** 12727-12731 (1993).
[59] A. R. Abramson, W. C. Kim, S. T. Huxtable, H. Q. Yan, Y. Y. Wu, A. Majumdar, C. L. Tien, and P. D. Yang, Journal of Microelectromechanical Systems **13,** 505-513 (2004).
[60] R. Venkatasubramanian, E. Siivola, T. Colpitts, and B. O'Quinn, Nature **413,** 597-602 (2001).
[61] D. Saha, A. D. Sharma, A. Sen, and H. S. Maiti, MATERIALS LETTERS **55,** 403-406 (2002).

[62] J. C. Kim, G. H. Park, S. J. Suh, Y. K. Lee, S. J. Lee, S. J. Lee, and J. D. Nam, Polymer Korea **26,** 367-374 (2002).
[63] C. S. Smith, Physical Review **94,** 42-49 (1954).
[64] G. Gerlach and R. Werthschutzky, Tm-Technisches Messen **72,** 53-76 (2005).
[65] S. M. Sze, *Physics of semiconductor devices*, 2nd ed. (Wiley, New York, USA, 1981).
[66] H. Jensenius, J. Thaysen, A. A. Rasmussen, L. H. Veje, O. Hansen, and A. Boisen, Applied Physics Letters **76,** 2615-2617 (2000).
[67] C. Stampfer, T. Helbling, D. Obergfell, B. Schoberle, M. K. Tripp, A. Jungen, S. Roth, V. M. Bright, and C. Hierold, Nano Letters **6,** 233-237 (2006).
[68] B. Naranjo, J. K. Gimzewski, and S. Putterman, Nature **434,** 1115-1117 (2005).
[69] R. Kohler, N. Neumann, N. Hess, R. Bruchhaus, W. Wersing, and M. Simon, Ferroelectrics **201,** 83-92 (1997).
[70] J. Lehman, E. Theocharous, G. Eppeldauer, and C. Pannell, Measurement Science & Technology **14,** 916-922 (2003).
[71] Q. Q. Zhang, H. L. W. Chan, and C. L. Choy, Computers part A-Applied Science and Manufacturing **30,** 163-167 (1999).
[72] L. Liang, Z. Liangying, and Y. Xi, Ceramics International **30,** 1843-1846 (2004).
[73] A. E. Clark and H. S. Belson, Physical Review B **5,** 3642-3644 (1972).
[74] M. Vazquez, M. Knobel, M. L. Sanchez, R. Valenzuela, and A. P. Zhukov, Sensors and Actuators A **59,** 20-29 (1997).
[75] T. R. McGuire and R. I. Potter, Ieee Transactions on Magnetics **11,** 1018-1038 (1975).
[76] M. N. Baibich, J. M. Broto, A. Fert, F. N. Vandau, F. Petroff, P. Eitenne, G. Creuzet, A. Friederich, and J. Chazelas, Physical Review Letters **61,** 2472-2475 (1988).
[77] G. Binasch, P. Grunberg, F. Saurenbach, and W. Zinn, Physical Review B **39,** 4828-4830 (1989).
[78] G. A. Prinz, Journal of Magnetism and Magnetic Materials **200,** 57-68 (1999).
[79] A. M. Fennimore, T. D. Yuzvinsky, W. Q. Han, M. S. Fuhrer, J. Cumings, and A. Zettl, Nature **424,** 408-410 (2003).
[80] K. Kurosawa, S. Yoshida, and K. Sakamoto, Journal of Lightwave Technology **13,** 1378-1384 (1995).
[81] D. M. Le Vine and S. Abraham, Ieee Transactions on Geoscience and Remote Sensing **40,** 771-782 (2002).
[82] J. Lenz and A. S. Edelstein, IEEE Sensors Journal **6,** 631-649 (2006).
[83] C. Hunt and S. Sahu, The IRM Quarterly **2,** 1-8 (1992).

[84] Z. Q. Qiu and S. D. Bader, Review of Scientific Instruments **71,** 1243-1255 (2000).
[85] Z. Q. Qiu and S. D. Bader, Journal of Magnetism and Magnetic Materials **200,** 664-678 (1999).
[86] W. J. Karl, A. L. Powell, R. Watts, M. R. J. Gibbs, and C. R. Whitehouse, Sensors and Actuators a-Physical **81,** 137-141 (2000).
[87] F. Tang, D. L. Liu, D. X. Ye, T. M. Lu, and G. C. Wang, Journal of Magnetism and Magnetic Materials **283,** 65-70 (2004).
[88] A. Yariv, *Optical electronics* (Oxford University Press, New York, USA, 1991).
[89] K. Hidaka, IEEE Electrical Insulation Magazine **12,** 17-23.
28 (1996).